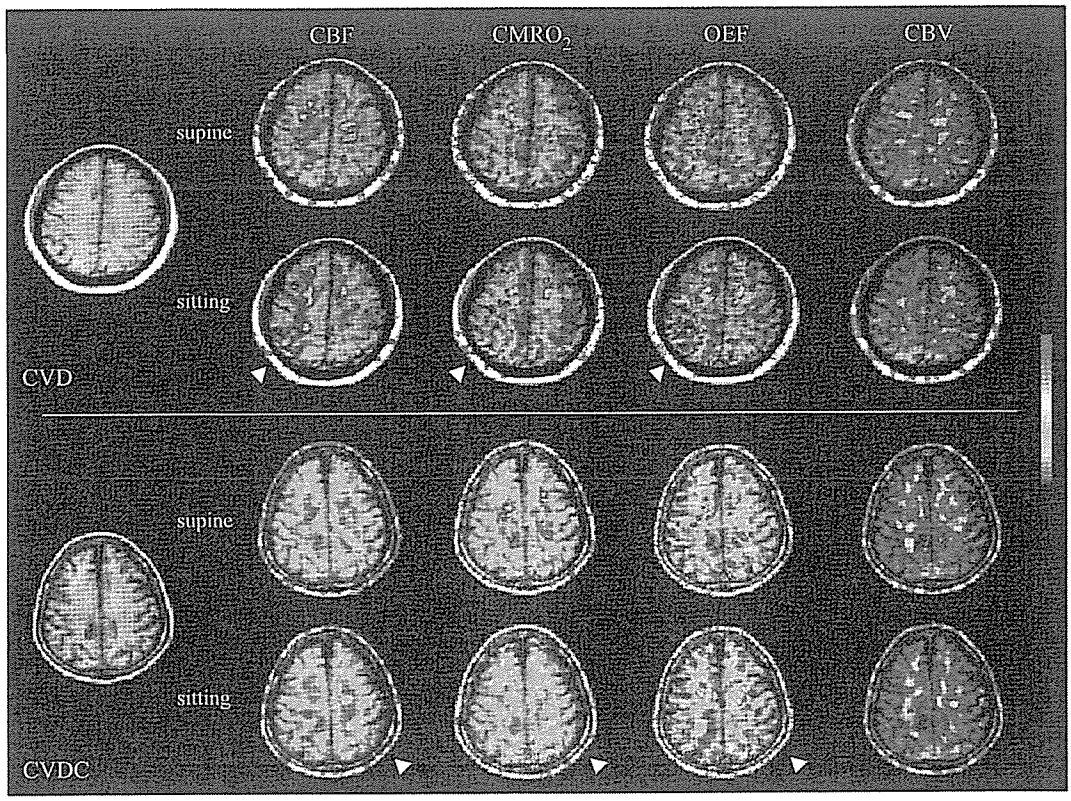

Fig. 5. PET images of a patient with right internal carotid occlusive disease (CVD) and one with left CVD plus coronary artery disease (CVDC) during supine and sitting postures. There were no abnormalities in the magnetic resonance images, but postural alterations in the hemodynamic and metabolic parameters were detected in the susceptible regions (arrowheads) in each disease group: reductions in CBF and $CMRO_2$ with slight increase in OEF in the CVDC group, and reduction in CBF with stable $CMRO_2$ and increase in OEF in the CVD group under the sitting condition.

caveats that must be taken, the timing of $CMRO_2$ acquisition was theoretically different from that of the CBF measurement in our study, and the PET data were acquired at least 15 min after the postural shift from the supine to sitting condition. These methodological limitations did not permit depiction of the dynamic phase of ongoing postural behavior and did not allow oxygen metabolism to be regarded as an independent measure from CBF, because $CMRO_2$ was quantified with the value of CBF. No significant changes in physiological parameters during the upright condition, however, could indicate the adequacy of handling CBF as a stable parameter during the upright condition, because the oxy/deoxy hemoglobin concentration reached a plateau 3 min after the

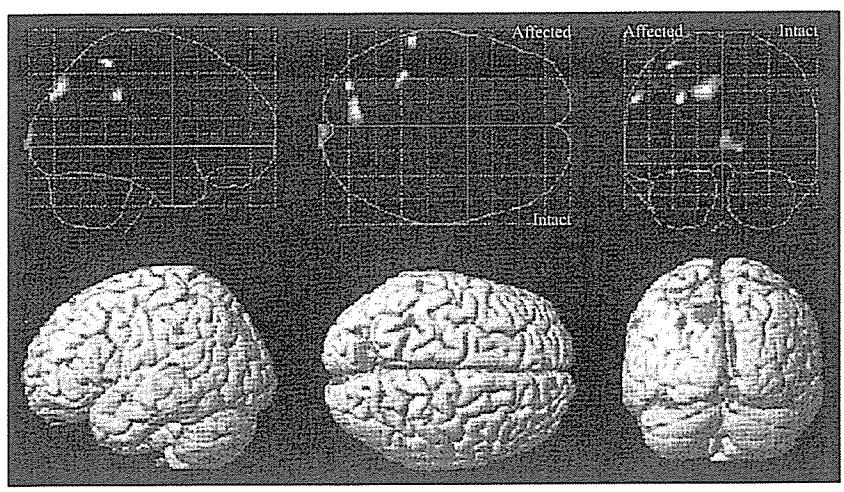

Fig. 6. SPM showed significant reduction in relative rCBF in the superior ($x\ y\ z = -34\ -46\ 60$, z score = 4.02) and inferior ($x\ y\ z = -58\ -40\ 36$, z score = 3.98) parietal lobules and precuneus ($x\ y\ z = -10\ -78\ 40$, z score = 4.38) on the occlusion side during sitting vs. lying ($P < 0.001$, uncorrected) in the disease group. The present result was similar to, but topographically different from, the previous result (Ouchi et al., 2001a,b), showing parietotemporal and frontal reductions in CBF. This discordance might be ascribed to differences in PET scanners used and in diseases analyzed (middle cerebral artery occlusion vs. ICAO).

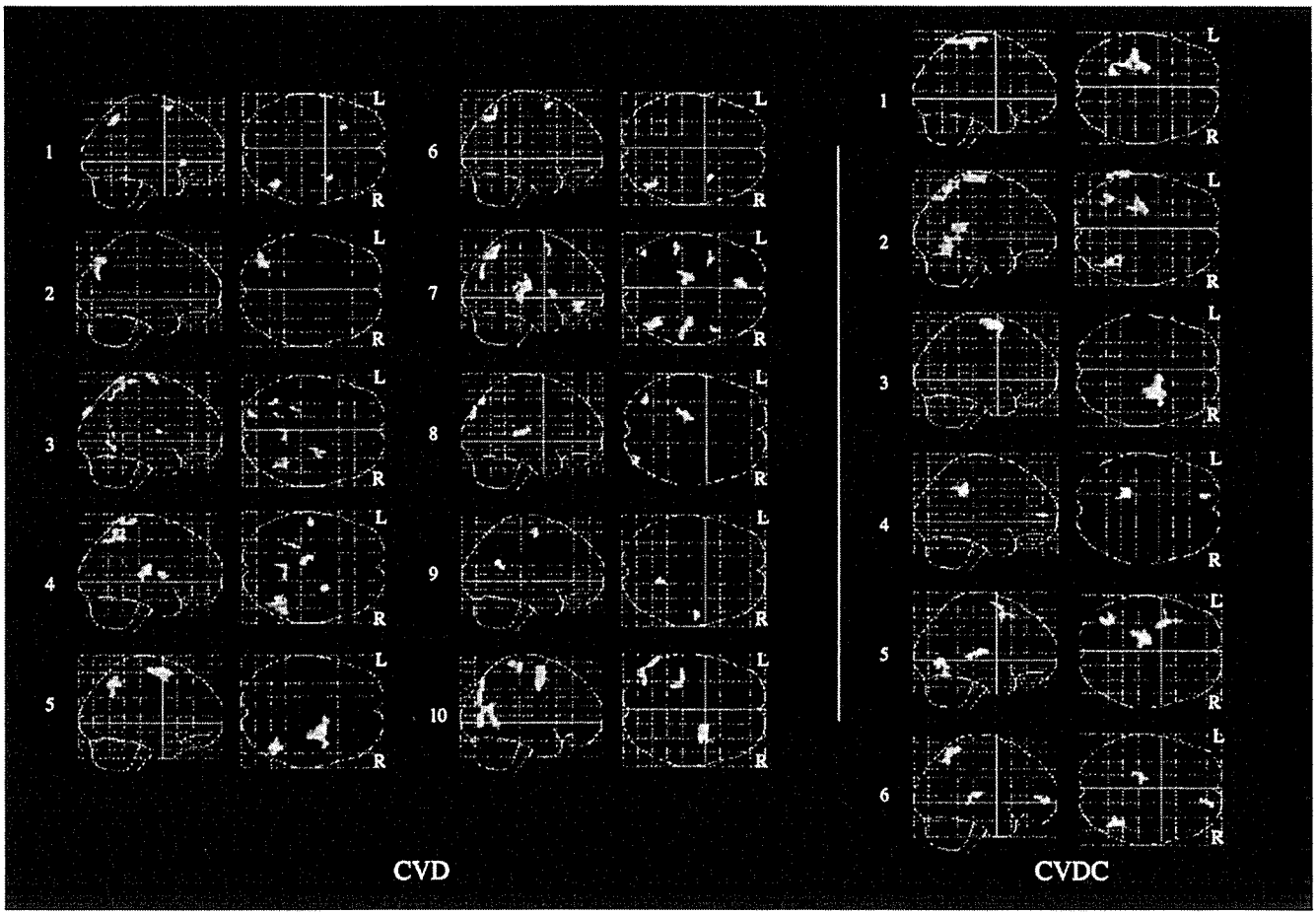

Fig. 7. Single-subject analysis for reduction in rCBF during sitting. The numbers of each glass brain correspond to the patient numbers seen in the Table 1. R, right; L, left.

postural change (Krakow et al., 2000). Although there were no significant differences in physiology among the three groups in the present study, it was not possible to determine the autonomic effect on the vasoneuronal and vasomuscular tones in the cerebral hemodynamics. Therefore, it is possible that there was a greater degree of implicit sympathetic effect that triggered a hemodynamic change in the coronary circulation (Muller, 1999) in the CVDC group, resulting in a reduction in cardiac output followed by a decrease in the cerebrovascular perfusion pressure.

The level of rCBF in the healthy group remained rather unchanged during the upright posture, which means that postural rCBF reduction might be ascribed to the impairment of local autoregulation in hemodynamically vulnerable regions in disease groups. This ABP-related CBF reduction was more significant in the affected-side parietal cortex in the CVDC group, and the relative metabolic demand was inversely augmented with MABP reduction (Fig. 4), suggesting that the susceptible ischemic region would require more energy to survive or maintain normal vasoreactivity for a further vascular dilatation event in CVD patients with cardiac ischemia. This speculation might be further supported by the present finding that a reduction in CBF/CBV correlated negatively with an increase in OEF and $CMRO_2$ in the frontal and parietal cortex distal to the affected region in the CVDC group (Fig. 3). The tendency of this negative correlation was also seen in the CVD group. In ischemic areas distal to an arterial occlusion, the arteriolar pressure has been considered to be much lower than that in the normal tissue and below the lower limit of autoregulation (Paulson, 1970; Shima et al., 1983; Symon et al., 1976). In the ischemic situation, the vascular (capillary-to-vein) pool or CBV has been considered to increase due to autoregulatory dilatation in the affected blood vessel to compensate for perfusion pressure reduction (Powers, 1991). Although a significant difference was not detected in the quantitative CBV level, due chiefly to large standard deviations (not shown) in the present study, the CBV tended to decrease in the vulnerable region during the upright posture, particularly in the CVDC group (Table 3). A recent PET study showed that acute administration of acetazolamide, a vasodilatory effect agent, resulted in an increase in the arterioler blood volume coupled with a rCBF reduction in those CVD patients with good collateral circulation (Okazawa et al., 2003). Thus, it was assumed that energy production might not be enough to make the arterioles respond to impending ischemic events when CVDC patients assume an upright posture. The lack of a decrease tendency of CBV in the CVD group might indicate that the vasodilatory capacity of arterioles in the ischemic region was sufficient.

From a clinical point of view, the incidence of ischemic stroke is at its maximum from eight to noon, the period of day during which blood pressure is at its highest in awake patients with stroke (Marler et al., 1989). The incidence of transient episodes of myocardial ischemia is also at a high point during this period (Muller, 1999). Thus, adequately controlling hypertension may be crucial for preventing the further development of stroke events for

patients when they are in an upright position. This issue is indeed important, because early introduction of active physical exercise after stroke is important for minimizing the long-term burdens of stroke (Hankey et al., 2002). During positive rehabilitation at an early stage, however, a fluctuation in neurological recovery has been reported to be occasionally encountered in patients with cardiovascular problems (Dromerick and Reding, 1994). In addition, acute recovery from cerebral ischemic attack was not considered a good sign, but, rather, an impending omen of subsequent neurological deterioration (Johnston et al., 2003). The present orthostatic PET measurement could provide one insight into the mechanism by which neurological deterioration on a molecular level develops in the susceptible brain region. However, the small sample size in the CVDC group would require a more extensive study for a number of patients with cardiac problems (symptomatic or asymptomatic), and hence the present result should be considered preliminary at this stage.

In conclusion, the current study demonstrated that upright posture caused local neural deactivation in the hemodynamically vulnerable brain region in patients with CVD. When the cardiac problem is accompanied by a CVD condition, the tissue oxygen demand would be increased with a decrease in perfusion pressure in the hemodynamically susceptible region, but a sufficient degree of net energy production might not be expected during the upright posture. The proper control of hypertension or drinking adequate amounts of water (Schroeder et al., 2002; Shannon et al., 2002) can reduce this insidious menace in CVD patients in general.

Acknowledgments

We would like to thank Dr. Teiji Nakyama, Dr. Masanobu Sakamoto, Dr. Kenichi Yano, Mr. Fumitoshi Nakamura, Ms. Tomomi Ogusu, and other staff in the Positron Medical Center for their advice and support on PET measurements. This study was supported by a grant from the Takeda Science Foundation.

References

Baron, J.C., Bousser, M.G., Rey, A., Guillard, A., Comar, D., Castaigne, P., 1981. Reversal of focal "misery-perfusion syndrome" by extra intracranial arterial bypass in hemodynamic cerebral ischemia. A case study with 15O positron emission tomography. Stroke 12, 454–459.

Daffertshofer, M., Diehl, R.R., Ziems, G.U., Hennerici, M., 1991. Orthostatic changes of cerebral blood flow velocity in patients with autonomic dysfunction. J. Neurol. Sci. 104, 32–38.

Derdeyn, C.P., Shaibani, A., Moran, C.J., Cross III, D.T., Grubb Jr., R.L., Powers, W.J., 1999. Lack of correlation between pattern of collateralization and misery perfusion in patients with carotid occlusion. Stroke 30, 1025–1032.

Dromerick, A., Reding, M., 1994. Medical and neurological complications during inpatient stroke rehabilitation. Stroke 25, 358–361.

Friston, K.J., Holmes, A.P., Worsley, K.J., Poline, J.P., Frith, C.D., Frackowiak, R.S.J., 1995. Statistical parametric mapping in functional imaging: a general linear approach. Hum. Brain Mapp. 2, 189–210.

Graafmans, W.C., Ooms, M.E., Hofstee, H.M., Bezemer, P.D., Bouter, L.M., Lips, P., 1996. Falls in the elderly: a prospective study of risk factors and risk profiles. Am. J. Epidemiol. 143, 1129–1136.

Hamar, J., Kovach, A.G., Reivich, M., Nyary, I., Durity, F., 1979. Effect of phenoxybenzamine on cerebral blood flow and metabolism in the baboon during hemorrhagic shock. Stroke 10, 401–407.

Hankey, G.J., Jamrozik, K., Broadhurst, R.J., Forbes, S., Anderson, C.S., 2002. Long-term disability after first-ever stroke and related prognostic factors in the Perth Community Stroke Study, 1989–1990. Stroke 33, 1034–1040.

Hayashida, K., Hirose, Y., Kaminaga, T., Ishida, Y., Imakita, S., Takamiya, M., et al., 1993. Detection of postural cerebral hypoperfusion with technetium-99 m-HMPAO brain SPECT in patients with cerebrovascular disease. J. Nucl. Med. 34, 1931–1935.

Herscovitch, P., Markham, J., Raichle, M.E., 1983. Brain blood flow measured with intravenous H215O. I. Theory and error analysis. J. Nucl. Med. 24, 782–789.

Johnston, S.C., Leira, E.C., Hansen, M.D., Adams, H.P.J., 2003. Early recovery after cerebral ischemia risk of subsequent neurological deterioration. Ann. Neurol. 54, 439–444.

Kapoor, W.N., 2000. Syncope. N. Engl. J. Med. 343, 1856–1862.

Krakow, K., Ries, S., Daffertshofer, M., Hennerici, M., 2000. Simultaneous assessment of brain tissue oxygenation and cerebral perfusion during orthostatic stress. Eur. Neurol. 43, 39–46.

Lakka, T.A., Salonen, R., Kaplan, G.A., Salonen, J.T., 1999. Blood pressure and the progression of carotid atherosclerosis in middle-aged men. Hypertension 34, 51–56.

Lammertsma, A.A., Jones, T., 1983. Correction for the presence of intravascular oxygen-15 in the steady-state technique for measuring regional oxygen extraction ratio in the brain: 1. Description of the method. J. Cereb. Blood Flow Metab. 3, 416–424.

Lammertsma, A.A., Baron, J.C., Jones, T., 1987. Correction for intravascular activity in the oxygen-15 steady-state technique is independent of the regional hematocrit. J. Cereb. Blood Flow Metab. 7, 372–374.

Levine, B.D., Giller, C.A., Lane, L.D., Buckey, J.C., Blomqvist, C.G., 1994. Cerebral versus systemic hemodynamics during graded orthostatic stress in humans. Circulation 90, 298–306.

Lipsitz, L.A., 1989. Orthostatic hypotension in the elderly. N. Engl. J. Med. 321, 952–957.

Mai, J.K., Assheuer, J., Paxinos, G., 1997. Atlas of the Human Brain. Academic Press, San Diego.

Marler, J.R., Price, T.R., Clark, G.L., Muller, J.E., Robertson, T., Mohr, J.P., et al. 1989. Morning increase in onset of ischemic stroke. Stroke 20, 473–476.

Mehagnoul-Schipper, D.J., Vloet, L.C., Colier, W.N., Hoefnagels, W.H., Jansen, R.W., 2000. Cerebral oxygenation declines in healthy elderly subjects in response to assuming the upright position. Stroke 31, 1615–1620.

Mintun, M.A., Raichle, M.E., Martin, W.R., Herscovitch, P., 1984. Brain oxygen utilization measured with O-15 radiotracers and positron emission tomography. J. Nucl. Med. 25, 177–187.

Muller, J.E., 1999. Circadian variation and triggering of acute coronary events. Am. Heart J. 137, S1–S8.

Muller, J.E., Tofler, G.H., Stone, P.H., 1989. Circadian variation and triggers of onset of acute cardiovascular disease. Circulation 79, 733–743.

Novak, V., Novak, P., Spies, J.M., Low, P.A., 1998. Autoregulation of cerebral blood flow in orthostatic hypotension. Stroke 29, 104–111.

Okazawa, H., Yamauchi, H., Sugimoto, K., Takahashi, M., 2003. Differences in vasodilatory capacity and changes in cerebral blood flow induced by acetazolamide in patients with cerebrovascular disease. J. Nucl. Med. 44, 1371–1378.

Ouchi, Y., Nobezawa, S., Okada, H., Yoshikawa, E., Futatsubashi, M., Kaneko, M., 1998. Altered glucose metabolism in the hippocampal head in memory impairment. Neurology 51, 136–142.

Ouchi, Y., Nobezawa, S., Yoshikawa, E., Futatsubashi, M., Kanno, T., Okada, H., et al., 2001a. Postural effects on brain hemodynamics in unilateral cerebral artery occlusive disease: a positron emission tomography study. J. Cereb. Blood Flow Metab. 21, 1058–1066.

Ouchi, Y., Okada, H., Yoshikawa, E., Futatsubashi, M., Nobezawa, S., 2001b. Absolute changes in regional cerebral blood flow in association with upright posture in humans: an orthostatic PET study. J. Nucl. Med. 42, 707–712.

Paulson, O.B., 1970. Regional cerebral blood flow in apoplexy due to occlusion of the middle cerebral artery. Neurology 20, 63–77.

Pitzalis, M., Massari, F., Guida, P., Iacoviello, M., Mastropasqua, F., Rizzon, B., et al., 2002. Shortened head-up tilting test guided by systolic pressure reductions in neurocardiogenic syncope. Circulation 105, 146–148.

Powers, W.J., 1991. Cerebral hemodynamics in ischemic cerebrovascular disease. Ann. Neurol. 29, 231–240.

Raiha, I., Luutonen, S., Piha, J., Seppanen, A., Toikka, T., Sourander, L., 1995. Prevalence, predisposing factors, and prognostic importance of postural hypotension. Arch. Intern. Med. 155, 930–935.

Schondorf, R., Benoit, J., Wein, T., 1997. Cerebrovascular and cardiovascular measurements during neurally mediated syncope induced by head-up tilt. Stroke 28, 1564–1568.

Schroeder, C., Bush, V.E., Norcliffe, L.J., Luft, F.C., Tank, J., Jordan, J., et al., 2002. Water drinking acutely improves orthostatic tolerance in healthy subjects. Circulation 106, 2806–2811.

Shannon, J.R., Diedrich, A., Biaggioni, I., Tank, J., Robertson, R.M., Robertson, D., et al., 2002. Water drinking as a treatment for orthostatic syndromes. Am. J. Med. 112, 355–360.

Shima, T., Hossmann, K.A., Date, H., 1983. Pial arterial pressure in cats following middle cerebral artery occlusion. 1. Relationship to blood flow, regulation of blood flow and electrophysiological function. Stroke 14, 713–719.

Strandgaard, S., Paulson, O.B., 1989. Cerebral blood flow and its pathophysiology in hypertension. Am. J. Hypertens. 2, 486–492.

Symon, L., Branston, N.M., Strong, A.J., 1976. Autoregulation in acute focal ischemia. An experimental study. Stroke 7, 547–554.

Warkentin, S., Passant, U., Minthon, L., Karlson, S., Edvinsson, L., Faldt, R., et al., 1992. Redistribution of blood flow in the cerebral cortex of normal subjects during head-up postural change. Clinic. Auton. Res. 2, 119–124.

Watanabe, M., Shimizu, K., Omura, T., Takahashi, M., Kosugi, T., Yoshikawa, E., et al., 2002. A new high resolution PET scanner dedicated to brain research. IEEE Trans. Nucl. Sci. 49, 634–639.

Yamauchi, H., Fukuyama, H., Kimura, J., Konishi, J., Kameyama, M., 1990. Hemodynamics in internal carotid artery occlusion examined by positron emission tomography. Stroke 21, 1400–1406.

Microglial Activation and Dopamine Terminal Loss in Early Parkinson's Disease

Yasuomi Ouchi, MD, PhD,[1] Etsuji Yoshikawa, BA,[2] Yoshimoto Sekine, MD, PhD,[1,2]
Masami Futatsubashi, BA,[2] Toshihiko Kanno, RT,[1] Tomomi Ogusu, MA,[2] Tatsuo Torizuka, MD, PhD[1]

Neuroinflammatory glial response may contribute to degenerative processes in Parkinson's disease (PD). To investigate changes in microglial activity associated with changes in the presynaptic dopamine transporter density in the PD brain in vivo, we studied 10 early-stage drug-naive PD patients twice using positron emission tomography with a radiotracer for activated microglia [^{11}C](*R*)-PK11195 and a dopamine transporter marker [^{11}C]CFT. Quantitative levels of binding potentials (BPs) of [^{11}C](*R*)-PK11195 and [^{11}C]CFT in the nigrostriatal pathway were estimated by compartment analyses. The levels of [^{11}C](*R*)-PK11195 BP in the midbrain contralateral to the clinically affected side were significantly higher in PD than that in 10 age-matched healthy subjects. The midbrain [^{11}C](*R*)-PK11195 BP levels significantly correlated inversely with [^{11}C]CFT BP in the putamen and correlated positively with the motor severity assessed by the Unified Parkinson's Disease Rating Scale in PD. In healthy subjects, the [^{11}C](*R*)-PK11195 BP in the thalamus and midbrain showed an age-dependent increase. In vivo demonstration of parallel changes in microglial activation and corresponding dopaminergic terminal loss in the affected nigrostriatal pathway in early PD supports that neuroinflammatory responses by intrinsic microglia contribute significantly to the progressive degeneration process of the disease and suggests the importance of early therapeutic intervention with neuroprotective drugs.

Ann Neurol 2005;57:168–175

The histopathological hallmarks of Parkinson's disease (PD) are the progressive degeneration of the nigral dopamine neurons and the ensuing loss of dopamine nerve terminals in the striatum.[1] Previous ex vivo and animal studies suggest that the loss of dopamine neurons is linked with an activation of microglia in the substantia nigra.[2–9] Neuropathological studies with 1-methyl-4-phenyl-1,2,3,6-tetrahydropyridine indicated that microglia might contribute to later and ongoing degeneration of nigral neurons.[10,11] Although these postmortem and animal studies have strongly suggested the relevance of microglial activation to the nigral cell death seen in PD patients, the antemortem relation between microglial expression and progressive loss of dopamine terminals in PD patients at an early stage remains unclear.

Microglia are involved in immune surveillance in the intact brain and become activated in response to inflammation, trauma, ischemia, tumor, and neurodegeneration.[12] A PD rat model with striatal lesions by 6-hydroxydopamine, secondarily causing retrograde damage to the nigral dopamine neurons, showed an increase in the binding of a specific marker for activated microglia, (1-(2-chrorophynyl)-*N*-methylpropyl)-3 isoquinoline carboxamide ([^{11}C]PK11195)[13,14] in the striatum and substantia nigra, which indicated an inflammatory response resulting from neural injury and/or neuronal death.[15] Based on use of the [^{11}C](*R*)-PK11195 enantiomer and positron emission tomography (PET), more detailed measurement of microglial activation in vivo recently has been reported in neurodegenerative disorders.[16,17] Furthermore, one of the dopamine transporter (DAT) markers, [^{11}C]2-B-carbomethoxy-3B-(4-fluorophenyl) tropane ([^{11}C]CFT), which allows us to depict the density of the dopaminergic terminals in PD patients in vivo, has shown a marked reduction in [^{11}C]CFT binding in the striatum in parallel with the severity of parkinsonism.[18–20] These in vivo imaging methods are advantageous in monitoring double aspects of progressively degenerated dopamine neurons, namely, alterations in neuroinflammatory reactions on the cell-body side and the resulting deletion of nerve terminals in the striatum.

For this purpose, we quantitatively measured the binding potentials (BPs) of [^{11}C](*R*)-PK11195 and [^{11}C]CFT in drug-naive patients with PD at an early stage on the same day because any delay in the measurement of the two tracers could obscure the accurate

From the [1]Positron Medical Center, Hamamatsu Medical Center; and [2]Central Research Laboratory, Hamamatsu Photonics K.K., Hamakita, Japan.

Received May 17, 2004, and in revised form Aug 13 and Oct 7. Accepted for publication Oct 7, 2004.

Published online Jan 26, 2005, in Wiley InterScience (www.interscience.wiley.com). DOI: 10.1002/ana.20338

Address correspondence to Dr Ouchi, Positron Medical Center, Hamamatsu Medical Center, 5000 Hirakuchi, Hamakita 434-0041, Japan. E-mail: ouchi@pmc.hmedc.or.jp

relation of ongoing neuroinflammation with neurodegeneration in the living brain.

Subjects and Methods

Participants

Ten drug-naive patients with PD rated at stage 1 to 2 on the Hoehn and Yahr scale (PD group, four men, six women; mean age, 59.6 years ± 9.9 standard deviation [SD]; range, 43–72) and 10 age-matched healthy subjects (N group, four men, six women; mean age, 53.1 years ± 12.5 SD; range, 39–70) participated in the present study. Patients who had been suffering from limb tremor, rigidity, and bradykinesia with a tentative clinical diagnosis as PD were recruited from our head hospital or the neighboring clinics, and the controls who were healthy physically and neurologically without any medication or complications were recruited by in-house advertisement. All participants underwent magnetic resonance imaging (MRI) and neurological and blood tests to exclude the possibility of any accompanying diseases. Diagnostic L-dopa treatment (L-dopa 100mg/day for 2–5 days) for all PD patients after PET examination markedly ameliorated their parkinsonian symptoms (reduction in frequency of tremor or disappearance of rigidity and bradykinesia). Clinical characteristics of PD patient are shown in Table 1. This study was approved by the ethics committee of the Hamamatsu Medical Center, and written informed consent was obtained from all participants after full explanation of the nature of the study.

Magnetic Resonance Imaging and Positron Emission Tomography Imaging

First, all participants underwent three-dimensional MRI just before the PET measurement. Here, we used a static magnet (0.3 T MRP7000AD; Hitachi, Tokyo, Japan) with three-dimensional mode sampling to determine the areas of the midbrain and the striatal nuclei required for setting the regions of interest (ROIs). The MRI measures and a mobile PET gantry allowed us to reconstruct PET images parallel to the intercommisural (anterior commissure–posterior commissure) line without reslicing; using this approach, we were able to allocate ROIs on the target regions of original PET images.[20]

PET scans were conducted with a high-resolution brain-purpose SHR12000 (Hamamatsu Photonics K.K., Hamamatsu, Japan) tomograph (intrinsic resolution, 2.9 × 2.9 ×3.4 full-width half-maximum [FWHM], 47 slices, 163mm axial field of view).[21] After the head fixation by a thermoplastic facemask and a 10-minute transmission scan for attenuation correction, serial scans (time frames: 4 × 30 seconds, 20 × 60 seconds, 14× 300 seconds) and periodical arterial blood sampling were performed for 92 minutes after a slow bolus injection (taking 1 minute) of a 350MBq dose of [^{11}C]CFT.[20,22] The [^{11}C](*R*)-PK11195 PET measurement then was performed after a 3-hour interval to allow for the decay of radioactivity. After the head was fixated at the same position as in the [^{11}C]CFT study, dynamic PET scans (4 × 30 seconds, 20 × 60 seconds, 8 × 300 seconds) were performed for 62 minutes without arterial blood sampling after intravenous injection of a 300MBq dose of [^{11}C](*R*)-PK11195.[14] The chronological order of the two PET studies was counterbalanced among the groups.

Image Data Analysis

Because gliosis is associated with changes in tissue volume,[16] a morphological study was first performed based on the previous volumetric MRI studies for midbrain morphology by measuring the maximum anteroposterior diameter of the midbrain through the substantia nigra and the maximum interpeduncular distance at the level of the substantia nigra and red nucleus on the MRIs.[23] Then, multiple semicircular ROIs (36~120mm^2) were drawn bilaterally over the midbrain (covering the substantia nigra, ventral tegmental area, and red nucleus), nucleus accumbens, ventromedial striatum (head of the caudate), the inferolateral (ventral putamen) and superodorsal parts (dorsal putamen) of the striatum, the thalamus, and the cerebellum on the MRIs.[24] These ROIs then were transferred onto the corresponding dynamic [^{11}C]CFT images and parametric images of [^{11}C](*R*)-PK11195 BP with 6.8mm slice-thickness data generated after adding two consecutive slices using image-processing software (Dr View;

Table 1. Clinical Characteristics of Parkinson's Disease Patients

Patient No.	Age (yr)	Sex	DD (yr)	H&Y	MMSE	UPDRS (me/act/mo)	Medication
1	56	M	1.6	2	29	4/4/10	Naive
2	43	M	0.9	1	29	2/4/5	Naive
3	65	M	0.8	2	29	3/6/9	Hypnotic/naive
4	72	M	1.8	2	29	4/6/11	Hypnotic/naive
5	58	F	2.5	1	30	2/4/6	Naive
6	70	F	1.2	1	27	3/8/15	Naive
7	57	F	1.9	2	27	3/6/20	Naive
8	71	F	0.9	1	29	3/4/8	Hypnotic/naive
9	48	F	0.4	1	28	2/5/9	Naive
10	56	F	1.9	2	26	4/12/11	Naive

Hypnotic medicines were temporarily used and stopped at least 1 week before position omission tomography measurement.
DD = disease duration; H&Y = modified Hoehn & Yahr disability score (1–5); MMSE = Mini-Mental State Examination (maximum = 30); UPDRS = Unified Parkinson's Disease Rating Scale (me = mentation, behavior, and mood; act = activities of daily living; mo = motor examination).

Asahi Kasei, Tokyo, Japan) on a SUN workstation (Hypersparc ss-20; SUN Microsystems, San Diego, CA).[25] The values of bilateral ROIs in the midbrain and cerebellum were averaged for further analysis.

[^{11}C](*R*)-PK11195 BP parametric images were generated according to the basis-function theory based on a simplified reference tissue model.[14,26] In this procedure, a normalized input curve was first created by averaging the ROIs placed over the cerebral cortical regions including the frontal, parietal, and occipital cortices in the healthy group. Then, we used this normalized mean tissue activity curve as the reference input function according to the cluster analysis theory[27] because a desirable reference region free of specific binding is not present in degenerative disorders, including PD. The population reference input curve (Fig 1, open circle) was used as the time activity curve (TAC) for the reference region. When applying this curve to the individual PD subjects, the normalized curve was calibrated by adjusting the cerebellar TAC peak from each PD patient. Instead of using the cluster segregation method,[14] the extracerebral structures were masked by demarcating cerebral regions on MRIs for further ROI analyses of PET images. Because, as described above, participants were scanned in the same position between the two PET measurements, the same ROIs could be placed on both [^{11}C]CFT and [^{11}C](*R*)-PK11195 parametric images. This approach allowed us to examine microglial activation in parallel with the degeneration of the presynaptic terminals in vivo. The binding potential (a ratio of binding and dissociation rate constants, k_3/k_4) for [^{11}C]CFT was analyzed based on the three-compartment model, as described elsewhere.[20,22]

Statistics

For between-group comparisons of [^{11}C]CFT and [^{11}C](*R*)-PK11195 binding levels, two-way analysis of variance (ANOVA) first was performed to assess BP levels with respect to one intersubject factor and the intrasubject factor (hemispheric side of the striatum) for evaluating the interhemispheric effect due to clinical manifestation of laterality in early PD. Because there was no significant interaction in the two-way ANOVA between the hemispheric side and types of groups ($p = 0.082$), all estimates were separately evaluated by one-way ANOVA in either region with Bonferroni's test for the correction of multiple comparisons. Statistical significance was given as p value less than 0.05 because the post hoc multiple comparisons were performed in these analyses. We previously have reported declines in [^{11}C]CFT binding associated with increases in age and in the severity of motor functions[20]; as such, simple linear regression analysis also was performed between age and [^{11}C](*R*)-PK11195 binding. In addition, Spearman's rank correlation analysis was performed to compare clinical motor scores of the Unified Parkinson's Disease Rating Scale with [^{11}C](*R*)-PK11195 binding levels in each region. The multiple regression analyses between regional [^{11}C]CFT binding and [^{11}C](*R*)-PK11195 binding were performed within each group. The level of significance was assumed to be p value less than 0.05.

Results

The Levels of [^{11}C]CFT and [^{11}C](R)-PK11195 Binding

The tissue TACs of [^{11}C](*R*)-PK11195 are shown in Figure 1. After administration of [^{11}C](*R*)-PK11195, the radioactivity in the midbrain and striatum of a healthy subject declined with time in the same fashion as the normalized mean TAC (population input curve) (see Fig 1A). In contrast, TAC of the midbrain in a

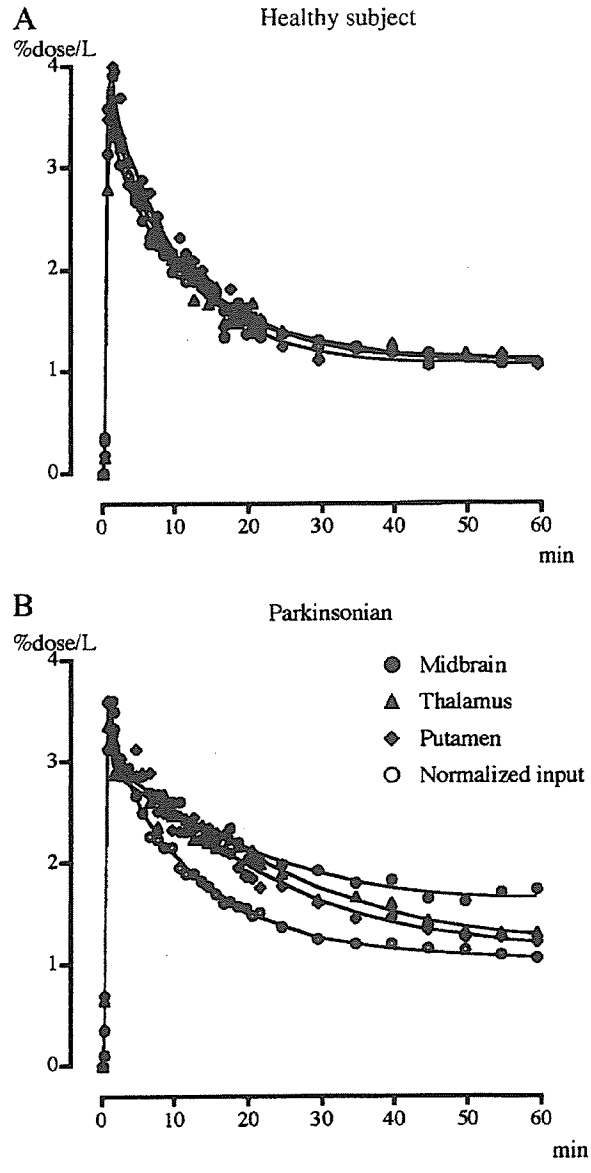

Fig 1. Regional tissue time-activity curves of [^{11}C](R)-PK11195 in a healthy subject (A) and a patient with Parkinson's disease (B). The normalized curve was generated as a reference input curve averaged from all the regions of interest values in the cerebral cortical regions without the midbrain, thalamus, and putamen in the healthy group.

Table 2. Levels of Binding Potential (k_3/k_4) for [^{11}C]CFT and [^{11}C]PK11195, Mean (SD)

Group	Tracer	DV_{CFT} / $R1_{PK}$ (Bilateral)	k_3/k_4									
			Midbrain Bilateral	Nucleus Accumbens		Caudate		Ventral Putamen		Dorsal Putamen		Thalamus	
				Ipsilateral	Contralateral	Ipsilateral	Contralateral	Ipsilateral	Contralateral	Ipsilateral	Contralateral	Ipsilateral	Contralateral
PD	CFT	7.86 (1.01)	ND	2.52 (0.97)	1.93[a](0.58)	2.37 (0.86)	2.04[a](0.85)	1.34[a](0.33)	1.18[a](0.27)	1.21[a](0.35)	0.83[a](0.24)	ND	ND
	PK	0.79 (0.06)	0.35[a](0.06)	<0.01	<0.01	0.08 (0.05)	0.01 (0.01)	0.04 (0.03)	0.03 (0.02)	<0.01	<0.01	0.12 (0.06)	0.13 (0.07)
N	CFT	7.95 (0.78)	—	2.95 (0.47)		3.92 (1.13)		4.44 (1.24)		3.64 (0.82)		ND	
	PK	0.74 (0.29)	0.11 (0.06)	0.06 (0.05)		0.04 (0.04)		0.07 (0.05)		0.06 (0.04)		0.10 (0.04)	

DV_{CFT} = distribution volume for the cerebellum in the [^{11}C]CFT measurement; $R1_{PK}$ = delivery index for the midbrain in the [^{11}C]PK11195 measurement; ND denotes not determined because of the negligible accumulation of [^{11}C]CFT.

[a] $p < 0.05$ vs normal group.

PD patient declined less sharply, indicating a time-course accumulation of [^{11}C](*R*)-PK11195 in the midbrain (see Fig 1B, closed circle). The statistics showed that midbrain values were significantly different from those of the thalamus and putamen after 40 minutes.

One-way ANOVA showed that the levels of k_3/k_4 for [^{11}C]CFT were significantly lower in all parts of the striatum ($p < 0.01$) in the PD group than those in the healthy group. The magnitude of k_3/k_4 in the PD group was lower in the dorsal putamen contralateral to the clinically more affected side (Table 2). No differences in distribution volume (DV) in the cerebellum of [^{11}C]CFT was found between the two groups. In the [^{11}C](*R*)-PK11195 study, the BP of the tracer was greater in the midbrain of the PD group than in the healthy counterparts (see Table 2), whereas there was no difference in the ratio of delivery (R_1) of the tracer between the target (midbrain) and reference tissue between the groups. The thalamus or striatum in PD failed to show any significant difference in binding. Morphometric measurement showed no significant differences in midbrain size (anteroposterior and transverse distances) between groups (Table 3), indicating no significant partial volume effect in further tracer analyses.

Correlations of [^{11}C](R)-PK11195 Binding with Age and Motor Severity in Parkinson's Disease Patients

Levels of [^{11}C](*R*)-PK11195 binding in the midbrain of the healthy group significantly correlated positively with age ($r = 0.68$; $p < 0.05$, f[x] = 0.0035*x − 0.073), whereas no such correlation was observed in the PD group (Fig 2A). This midbrain [^{11}C](*R*)-PK11195 binding in the PD group significantly correlated positively with the motor severity of the UPRDS assessment ($r = 0.74$; $p < 0.05$, f[x] = 0.012*x + 0.19; see Fig 2B) but failed to show a significant correlation against the disease duration ($r = 0.36$, $p > 0.1$; see Fig 2C). The examined brain regions other than the midbrain showed no significant correlation between [^{11}C](*R*)-PK11195 binding and motor scores in either group (not shown).

Comparison between Binding Levels of Striatal [^{11}C]CFT and Midbrain [^{11}C](R)-PK11195 in Parkinson's Disease Patients

Regression analyses showed that estimates for [^{11}C](*R*)-PK11195 binding in the midbrain significantly correlated negatively with those for [^{11}C]CFT binding in the dorsal putamen contralateral to the affected side ($r = 0.894$; $p < 0.01$, f[x] = −4.18*x + 2.30) and its ipsilateral counterpart ($r = 0.72$, $p < 0.05$, f(x)= −3.94*x + 2.59; Fig 3C). There was a tendency toward a negative correlation in the caudate ($p > 0.05$; see Fig 3A).

Discussion

Theses results showed to our knowledge for the first time with PET markers a higher accumulation of [^{11}C](*R*)-PK11195 in the midbrain in drug-naive early PD patients than in age-matched healthy subjects in vivo. In addition, the levels of midbrain [^{11}C](*R*)-PK11195 binding correlated negatively with the levels of [^{11}C]CFT binding in the putamen in the PD group. These results suggest that microglial activation was more significant in patients with more severe damage in the nigrostriatal pathway. This contention was supported by the results from the PD rat model showing the chronological decrease in [^{11}C]CFT accumulation in the lesioned striatum along with a parallel increase in [^{11}C](*R*)-PK11195 in the substantia nigra,[15] and from the postmortem analysis of the 1-methyl-4-phenyl-1,2,3,6-tetrahydropyridine–intoxicated human sub-

Table 3. Magnetic Resonance Imaging–based Midbrain Linear Measurements (cm), Mean (SD)[a]

Group	Antreroposterior Diameter	Interpeducular Distance
Parkinson's disease	26.5 (1.9)	36.8 (4.1)
Normal	27.6 (2.7)	37.4 (1.7)

There were no significant differences in measures between groups ($p > 0.05$, one-way analysis of variance).

[a] Results are maximum values of each distance.

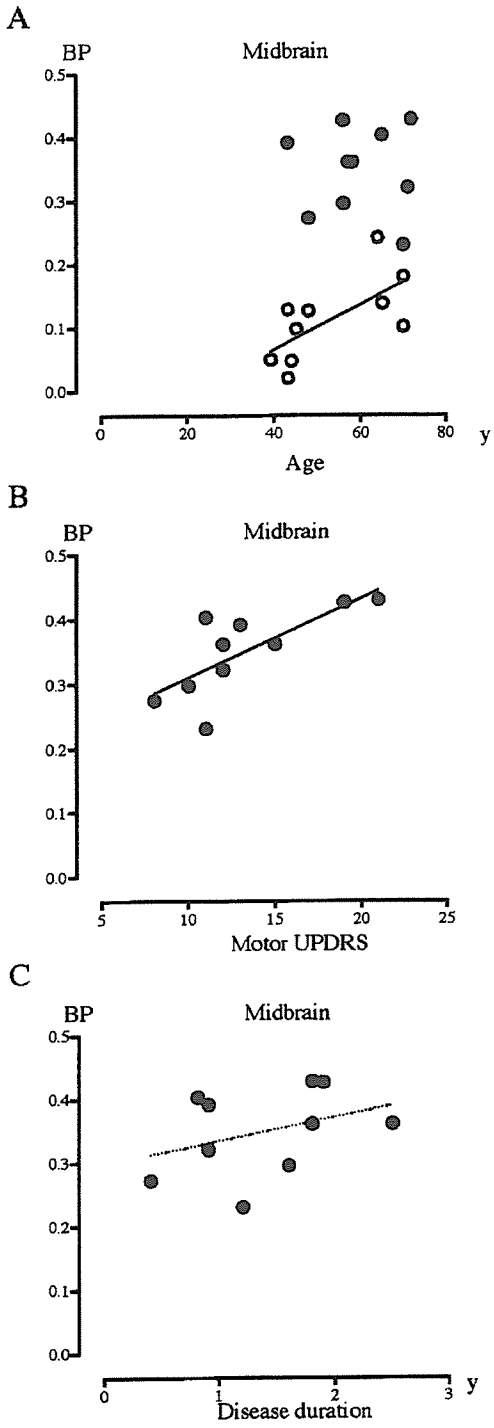

Fig 2. Correlations between levels of [^{11}C](R)-PK11195 binding in the midbrain and age (A) in the healthy group (open circles) *and Parkinson's disease group* (filled circles), *and motor scores of Unified Parkinson's Disease Rating Scale (UPDRS) (B) , and disease duration (year) (C) in the Parkinson's disease group. BP = binding potential.*

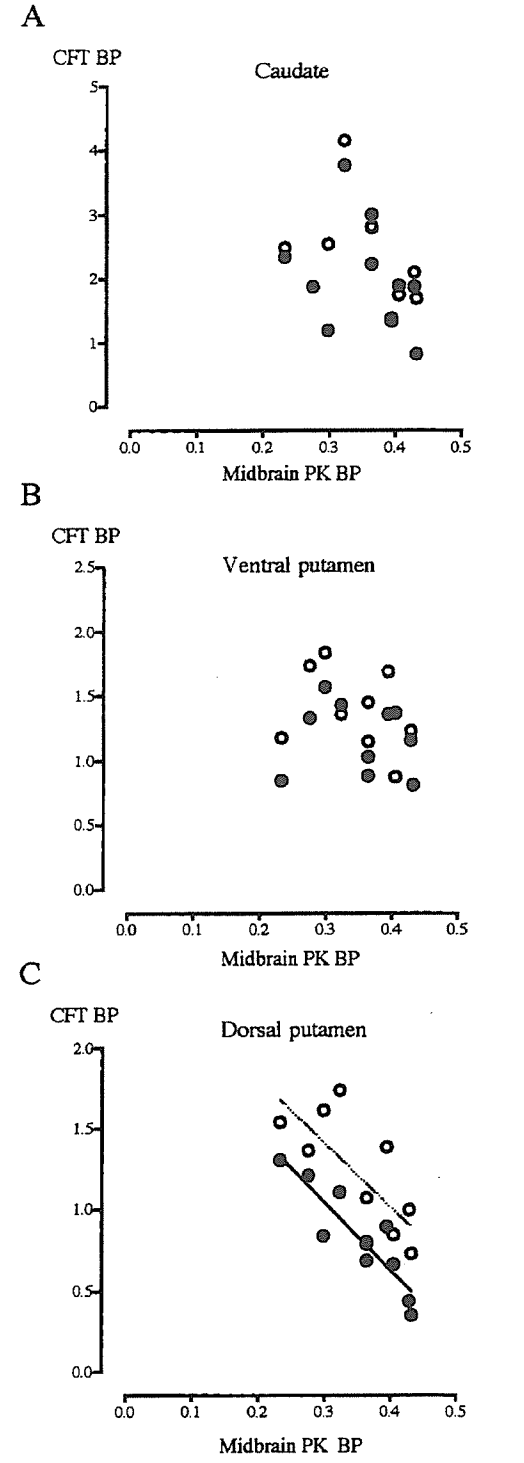

Fig 3. Correlations between levels of [^{11}C](R)-PK11195 binding potential (BP) in the midbrain and those of [^{11}C]CFT BP in the caudate (A), ventral putamen (B), and dorsal putamen (C) ipsilateral (open circles) *and contralateral* (filled circles) *to the clinically more affected side in the Parkinson's disease group.*

jects showing both elevated glial reaction in the substantia nigra and the dopaminergic neuronal loss.[10] Thus, our in vivo observation is compatible with the contention that microglial activation plays a key role in the initiation and progression of PD.

With respect to the role of microglia, there are lines of evidence that the majority of factors produced by activated microglia such as the cytokines tumor necrosis factor–α, interleukin-1β, and free radicals are proinflammatory or neurotoxic,[28–30] which suggests that activation of microglia would trigger the onset of a cascade of events resulting in a progressive degeneration of dopamine neurons. Although the age-related increase in [^{11}C](*R*)-PK11195 binding seen in healthy subjects in this study was not present in the PD group (see Fig 2A), it is likely that the degree of microglical activation associated with the disease is so great that it simply dwarfs the effect of aging. An age-related change in [^{11}C](*R*)-PK11195 binding in the thalamus in healthy subjects (data not shown) was also observed, as reported elsewhere.[16,31] These age-associated increases in microglial expression in the thalamus and midbrain may be related to the steady decline in higher cognitive and motor functions in normal aging that would jeopardize functional integration of the basal ganglia-cerebral cortical network. A lack of correlation of microglial activation with the disease duration (see Fig 2C) in this study suggested that the microglial reactive process might not be in parallel to the disease deterioration. To further illuminate this issue, this type of in vivo imaging on a chronological basis would be necessary.

There are a few methodological considerations to be noted in this study. First, PET has a critical limitation regarding image resolution for tiny structures such as the substantia nigra in the midbrain. A higher image resolution would enable us to elucidate the relation between microglial activation and dopaminergic neuronal loss in both nigrostriatal and mesolimbic (via the nucleus accumbens) systems by placing ROIs in those subregions of the midbrain. However, as shown in Figure 4, a greater degree of [^{11}C](*R*)-PK11195 binding tended to be observed in the midbrain contralateral to the clinically more affected side. Second, our tracer kinetic modeling was based on the reference tissue model,[26] and determination of normal reference tissue input was derived from the averaged value from the cerebral cortical regions in the 12 healthy subjects. Slightly lower levels of [^{11}C](*R*)-PK11195 binding in each of the brain regions examined in our study than the reported values[14,16] might be ascribed to the different methodological approach. However, the ratios of

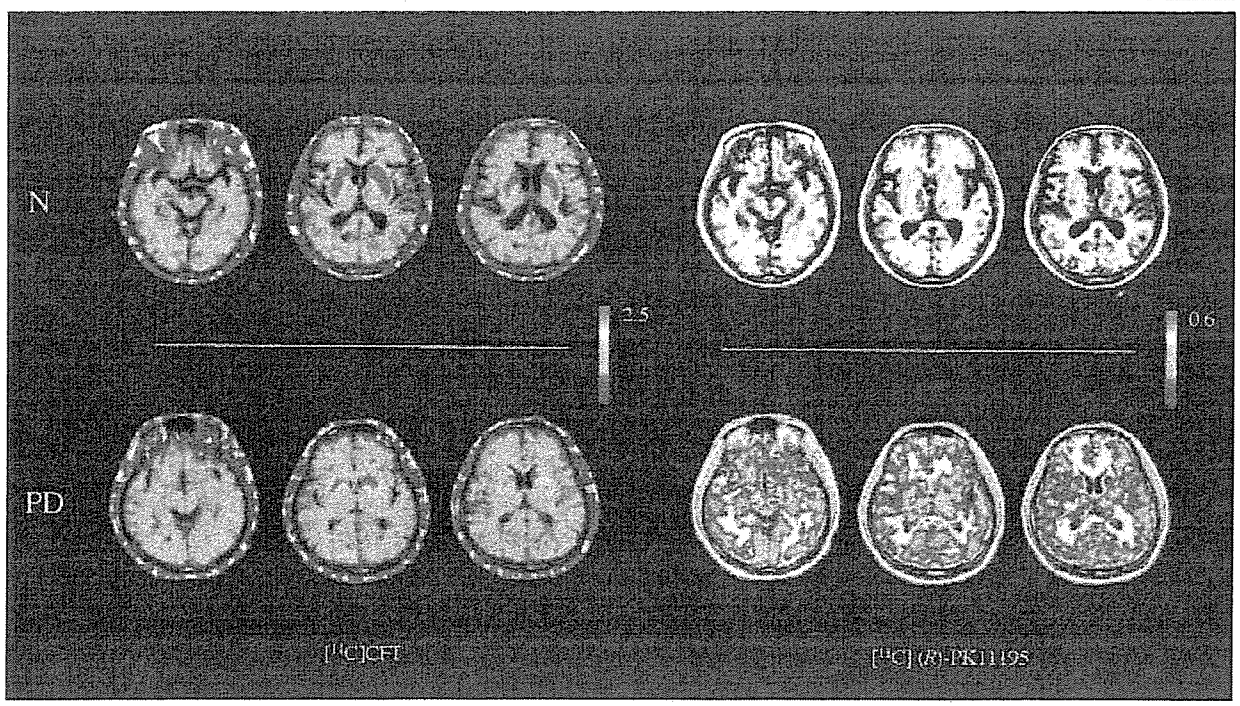

Fig 4. Magnetic resonance imaging positron emission tomography fusion parametric images of [^{11}C]CFT accumulation normalized to the cerebellum and [^{11}C](R)-PK11195 binding potential in a healthy subject (N) and a Parkinson's disease patient (PD) rated as Hoehn & Yahr stage 2. A marked increase in [^{11}C](R)-PK11195 binding was observed in the midbrain contralateral to the more disabled side along with a reduction in [^{11}C]CFT uptake in the putamen in the PD patient. For each tracer, red represents the highest value and dark violet represents the lowest value.

disease levels to control levels were fairly similar to those previously reported.

It has been reported that in PD, neuronal loss starts in the lateral ventral tier of the substantia nigra that projects to the dorsal putamen, and hence dopamine in the dorsal zone was more depleted than in the ventral zone in early PD.[1] This topological evidence supports our finding of a correlation between the increased [^{11}C](*R*)-PK11195 accumulation in the midbrain and the decreased accumulation of [^{11}C]CFT in the dorsal putamen (see Fig 3C). A more robust negative correlation was found clinically in the dorsal putamen contralateral to the more affected side. Interestingly, this nigral [^{11}C](*R*)-PK11195 accumulation was significantly correlated positively with motor severity in the present PD group (see Fig 2B). In contrast with the tegmental area or the medial tier of the substantia nigra projecting to the limbocortical region or the caudate (linking with mental and cognitive activities), because this dorsal putamen is considered to engage in motor execution,[32,33] this finding would reinforce the idea that the occurrence of microglial activation in the midbrain of PD at an early stage reflects dopamine loss sufficient to cause clinical parkinsonism.

From a therapeutic perspective, it was reported that antiinflammatory steroids,[34] nonsteroidal cyclooxygenase inhibitors,[35] and opioid receptor antagonist naloxone [36] might be promising as antiinflammatory agents for degenerative diseases such as PD. One epidemiological study agreed with the idea that use of nonsteroidal antiinflammatory drugs can delay the onset of PD.[37] In contrast, other clinical studies showed lesser effects of antiinflammatory drugs on a deceleration of the prevalence of PD than that in Alzheimer's disease[38,39] and therapeutic inconsistencies was suspected between laboratory data and clinical outcomes.[40] This result showing microglial activation along with dopaminergic terminal loss in vivo in early PD might afford a scope of discussion for use of the antiinflammatory and neuroprotective agents.

In conclusion, this study supports the contention that microglial activation develops in the midbrain of PD patients at an early stage, and that this appearance may be associated with likely ensuing apoptotic events. The latter issue must be clarified by a chronological study, but the present, one-time, double-tracer study for targeting both neuroinflammation and neuronal loss in the nigrostriatal system provides essential information about the degeneration process in PD.

We thank all patients and healthy subjects who participated in this study, Dr K. Tanaka and Dr M. Sakamoto for patients' selection, H. Okada for his constant technical support, Dr Y. Magata for his valuable advice on radiocompound syntheses, and our staff for support of the present PET study.

References

1. Kish SJ, Shannak K, Hornykiewicz O. Uneven pattern of dopamine loss in the striatum of patients with idiopathic Parkinson's disease. Pathophysiologic and clinical implications. N Engl J Med 1988;318:876–880.
2. McGeer PL, Itagaki S, Akiyama H, McGeer EG. Rate of cell death in parkinsonism indicates active neuropathological process. Ann Neurol 1988;24:574–576.
3. McGeer PL, Itagaki S, Boyes BE, McGeer EG. Reactive microglia are positive for HLA-DR in the substantia nigra of Parkinson's and Alzheimer's disease brains. Neurology 1988;38: 1285–1291.
4. Mirza B, Hadberg H, Thomsen P, Moos T. The absence of reactive astrocytosis is indicative of a unique inflammatory process in Parkinson's disease. Neuroscience 2000;95:425–432.
5. Vila M, Jackson-Lewis V, Guegan C, et al. The role of glial cells in Parkinson's disease. Curr Opin Neurol 2001;14: 483–489.
6. Akiyama H, McGeer PL. Microglial response to 6-hydroxydopamine-induced substantia nigra lesions. Brain Res 1989; 489:247–253.
7. Gao HM, Jiang J, Wilson B, et al. Microglial activation-mediated delayed and progressive degeneration of rat nigral dopaminergic neurons: relevance to Parkinson's disease. J Neurochem 2002;81:1285–1297.
8. Sherer TB, Betarbet R, Kim JH, Greenamyre JT. Selective microglial activation in the rat rotenone model of Parkinson's disease. Neurosci Lett 2003;341:87–90.
9. Sugama S, Yang L, Cho BP, et al. Age-related microglial activation in 1-methyl-4-phenyl-1,2,3,6-tetrahydropyridine (MPTP)-induced dopaminergic neurodegeneration in C57BL/6 mice. Brain Res 2003;964:288–294.
10. Langston JW, Forno LS, Tetrud J, et al. Evidence of active nerve cell degeneration in the substantia nigra of humans years after 1-methyl-4-phenyl-1,2,3,6 tetrahydropyridine exposure. Ann Neurol 1999;46:598–605.
11. McGeer PL, Schwab C, Parent A, Doudet D. Presence of reactive microglia in monkey substantia nigra years after 1-methyl-4-phenyl-1,2,3,6-tetrahydropyridine administration. Ann Neurol 2003;54:599–604.
12. Kreutzberg GW. Microglia: a sensor for pathological events in the CNS. Trends Neurosci 1996;19:312–318.
13. Conway EL, Gundlach AL, Craven JA. Temporal changes in glial fibrillary acidic protein messenger RNA and [3H]PK11195 binding in relation to imidazoline-I2-receptor and alpha 2-adrenoceptor binding in the hippocampus following transient global forebrain ischaemia in the rat. Neuroscience 1998;82: 805–817.
14. Banati RB, Newcombe J, Gunn RN, et al. The peripheral benzodiazepine binding site in the brain in multiple sclerosis: quantitative in vivo imaging of microglia as a measure of disease activity. Brain 2000;123:2321–2337.
15. Cicchetti F, Brownell AL, Williams K, et al. Neuroinflammation of the nigrostriatal pathway during progressive 6-OHDA dopamine degeneration in rats monitored by immunohistochemistry and PET imaging. Eur J Neurosci 2002;15:991–998.
16. Cagnin A, Brooks DJ, Kennedy AM, et al. In-vivo measurement of activated microglia in dementia. Lancet 2001;358: 461–467.
17. Banati RB. Visualising microglial activation in vivo. Glia 2002; 40:206–217.
18. Frost JJ, Rosier AJ, Reich SG, et al. Positron emission tomographic imaging of the dopamine transporter with 11C-WIN 35,428 reveals marked declines in mild Parkinson's disease. Ann Neurol 1993;34:423–431.

19. Wullner U, Pakzaban P, Brownell AL, et al. Dopamine terminal loss and onset of motor symptoms in MPTP-treated monkeys: a positron emission tomography study with 11C-CFT. Exp Neurol 1994;126:305–309.
20. Ouchi Y, Yoshikawa E, Okada H, et al. Alterations in binding site density of dopamine transporter in the striatum, orbitofrontal cortex, and amygdala in early Parkinson's disease: compartment analysis for beta-CFT binding with positron emission tomography. Ann Neurol 1999;45:601–610.
21. Watanabe M, Shimizu K, Omura T, et al. A new high resolution PET scanner dedicated to brain research. IEEE Trans Nucl Sci 2002;49:634–639.
22. Wong DF, Yung B, Dannals RF, et al. In vivo imaging of baboon and human dopamine transporters by positron emission tomography using [11C]WIN 35,428. Synapse 1993;15: 130–142.
23. Doraiswamy PM, Na C, Husain MM, et al. Morphometric changes of the human midbrain with normal aging: MR and stereologic findings. AJNR Am J Neuroradiol 1992;13: 383–386.
24. Mai JK, Assheuer J, Paxinos G. Atlas of the human brain. San Diego: Academic Press, 1997.
25. Ouchi Y, Kanno T, Okada H, et al. Presynaptic and postsynaptic dopaminergic binding densities in the nigrostriatal and mesocortical systems in early Parkinson's disease: a double-tracer positron emission tomography study. Ann Neurol 1999; 46:723–731.
26. Lammertsma AA, Bench CJ, Hume SP, et al. Comparison of methods for analysis of clinical [11C]raclopride studies. J Cereb Blood Flow Metab 1996;16:42–52.
27. Gun R, Lammertsma AA, Cunningham VJ. Parametric imaging of ligand-receptor binding in PET using a simplified reference tissue model and cluster analysis. In: Carson R, Daule M, Witherspoon P, Herscovitch P, eds. Quantitative functional brain imaging with PET. San Diego, CA: Academic Press, 1998:401–406.
28. Boje KM, Arora PK. Microglial-produced nitric oxide and reactive nitrogen oxides mediate neuronal cell death. Brain Res 1992;587:250–256.
29. Ehrlich LC, Hu S, Sheng WS, et al. Cytokine regulation of human microglial cell IL-8 production. J Immunol 1998;160: 1944–1948.
30. McGuire SO, Ling ZD, Lipton JW, et al. Tumor necrosis factor alpha is toxic to embryonic mesencephalic dopamine neurons. Exp Neurol 2001;169:219–230.
31. Banati RB, Cagnin A, Brooks DJ, et al. Long-term trans-synaptic glial responses in the human thalamus after peripheral nerve injury. Neuroreport 2001;12:3439–3442.
32. Ouchi Y, Yoshikawa E, Futatsubashi M, et al. Effect of simple motor performance on regional dopamine release in the striatum in parkinson disease patients and healthy subjects: a positron emission tomography study. J Cereb Blood Flow Metab 2002;22:746–752.
33. Goerendt IK, Messa C, Lawrence AD, et al. Dopamine release during sequential finger movements in health and Parkinson's disease: a PET study. Brain 2003;126:312–325.
34. Castano A, Herrera AJ, Cano J, Machado A. The degenerative effect of a single intranigral injection of LPS on the dopaminergic system is prevented by dexamethasone, and not mimicked by rh-TNF-alpha, IL-1beta and IFN-gamma. J Neurochem 2002;81:150–157.
35. Lipsky PE. The clinical potential of cyclooxygenase-2-specific inhibitors. Am J Med 1999;106:51S–57S.
36. Liu B, Hong JS. Role of microglia in inflammation-mediated neurodegenerative diseases: mechanisms and strategies for therapeutic intervention. J Pharmacol Exp Ther 2003;304:1–7.
37. Chen H, Zhang SM, Hernan MA, et al. Nonsteroidal anti-inflammatory drugs and the risk of Parkinson disease. Arch Neurol 2003;60:1059–1064.
38. McGeer PL, Schulzer M, McGeer EG. Arthritis and anti-inflammatory agents as possible protective factors for Alzheimer's disease: a review of 17 epidemiologic studies. Neurology 1996;47:425–432.
39. Czlonkowska A, Kurkowska-Jastrzebska I, Czlonkowski A, et al. Immune processes in the pathogenesis of Parkinson's disease—a potential role for microglia and nitric oxide. Med Sci Monit 2002;8:RA165–RA177.
40. Schapira AH, Olanow CW. Neuroprotection in Parkinson disease: mysteries, myths, and misconceptions. JAMA 2004; 291:358–364.

Neuropsychopharmacology (2004) 29, 1019–1026

www.neuropsychopharmacology.org

Metabolite Alterations in Basal Ganglia Associated with Psychiatric Symptoms of Abstinent Toluene Users: A Proton MRS Study

Kiyokazu Takebayashi[1], Yoshimoto Sekine[1], Nori Takei*[,1,2,3], Yoshio Minabe[1], Haruo Isoda[4], Hiroyasu Takeda[4], Katsuhiko Nishimura[1], Kazuhiko Nakamura[1], Katsuaki Suzuki[1], Yasuhide Iwata[1], Harumi Sakahara[4] and Norio Mori[1]

[1]Department of Psychiatry and Neurology, Hamamatsu University School of Medicine, Hamamatsu, Shizuoka, Japan; [2]Stanley Foundation Research Center in Japan, Hamamatsu, Shizuoka, Japan; [3]Department of Psychological Medicine, Institute of Psychiatry, London, UK; [4]Department of Radiology, Hamamatsu University School of Medicine, Hamamatsu, Shizuoka, Japan

Long-term toluene abuse causes a variety of psychiatric symptoms. However, little is known about abnormalities at the neurochemical level in the living human brain after long-term exposure to toluene. To detect neurochemical changes in the basal ganglia of subjects with a history of long-term toluene use, proton magnetic resonance spectroscopy (^{1}H MRS) was performed in 12 abstinent toluene users and 13 healthy comparisons with no history of drug abuse. *N*-acetylaspartate (NAA), creatine plus phosphocreatine (Cr + PCr), choline-containing compounds (Cho), and myo-inositol (MI) levels were measured in the left and right basal ganglia. The Cho/Cr + PCr ratio, a marker of membrane metabolism, was significantly increased in the basal ganglia of toluene users in comparison to that of the control subjects. Furthermore, the increase in the Cho/Cr + PCr ratio was significantly correlated with the severity of residual psychiatric symptoms. These findings suggest that long-term toluene use causes membrane disturbance in the basal ganglia, which is associated with residual psychiatric symptoms that persist even after long-term abstinence from toluene use.
Neuropsychopharmacology (2004) **29,** 1019–1026, advance online publication, 24 March 2004; doi:10.1038/sj.npp.1300426

Keywords: toluene-related symptoms; proton magnetic resonance spectroscopy; basal ganglia

INTRODUCTION

Organic solvent abuse is a worldwide problem, particularly among adolescents (Flanagan and Ives, 1994; Neumark *et al*, 1998). The easy accessibility to organic solvents makes them among the first drugs tried by teenagers. Consequently, teenagers are liable to develop an addiction to organic solvents, and such use can serve as a 'gateway' to the ingestion of other illicit drugs (Ives, 2000). Toluene is one of the major components of many organic solvents and is highly lipid-soluble (Morton, 1987). Toluene rapidly permeates lipid-rich regions of the body such as the brain, and its recreational intake can cause chronic and persistent psychiatric symptoms, including hallucinations and alterations in personality, even after cessation of toluene use (Hormes *et al*, 1986; Morton, 1987). However, the mechanisms responsible for these residual psychiatric symptoms following chronic toluene use remain unknown.

In experimental animal studies, exposure to toluene has been shown to produce changes in lipid membrane fluidity and membrane function (Kyrklund *et al*, 1987; LeBel and Schatz, 1990; von Euler *et al*, 1990). Furthermore, long-term exposure to toluene induces a persistent dopaminergic dysfunction in the rat basal ganglia, and this toluene-induced dopaminergic dysfunction has been related to the behavioral changes and the persistent cognitive deficits in rats (Cintra *et al*, 1999; Hillefors-Berglund *et al*, 1995; von Euler *et al*, 1993, 2000).

In human MR studies of toluene users, T2-weighted magnetic resonance images revealed global atrophy in the cerebrum, cerebellum, and brainstem (Rosenberg *et al*, 1988). Loss of differentiation between gray and white matter, increased periventricular white matter signal intensity (Aydin *et al*, 2002; Filley *et al*, 1990; Rosenberg *et al*, 1988, 2002), and hypointensity in the thalamus and

*Correspondence: Dr N Takei, Department of Psychiatry and Neurology, Hamamatsu University School of Medicine, 1-20-1 Handayama, Hamamatsu, 431-3192 Shizuoka, Japan, Tel: +81 53 435 2295, Fax: +81 53 435 3621,
E-mail address: ntakei@hama-med.ac.jp
Received 04 August 2003; revised 23 January 2004; accepted 27 January 2004
Online publication: 5 February 2004 at http://www.acnp.org/citations/Npp02050403349/default.pdf

basal ganglia (Rosenberg *et al*, 2002; Unger *et al*, 1994) have also been found in toluene users. Furthermore, white matter changes have been reported to be associated with neurocognitive deficits in long-term toluene users (Filley *et al*, 1990). However, little is known about the effects of long-term toluene use on the human brain at the neurochemical level.

Proton magnetic resonance spectroscopy (^{1}H MRS) offers an opportunity to evaluate *in vivo* neurochemical changes that might occur in toluene users. In this study, we investigated the potential of ^{1}H MRS scanning for revealing neurochemical changes in the chemistry of the basal ganglia of abstinent toluene users; we also considered whether or not such changes, if found, could possibly be related to the clinical characteristics observed in abstinent toluene users.

METHODS

Subjects

A total of 12 toluene users and 13 healthy comparison subjects who had never used toluene were recruited for our comprehensive research project on substance-related psychiatric disorders. Candidates were excluded if they were seropositive for human immunodeficiency virus type-1 (HIV-1), if they had a history of head trauma with loss of consciousness, or if they had brain morphological abnormalities (eg atrophy or tumor, etc) on MR images. All participants showed no neurological abnormalities and had no history of stupor or coma, which may be observed during intoxication after the use of high doses of toluene. All subjects were screened using the Structured Clinical Interview for DSM-IV (SCID) (First *et al*, 1996). More specifically, detailed information on toluene use and the history of psychiatric symptoms was retrospectively obtained from the toluene users; SCID-based interviews with the users and their family members were conducted, and patient medical records were considered as well. None of the toluene users had used any other drugs (ie they were mono-drug users) and the subjects had had no history of DSM-IV mental disorders before the use of toluene. The comparison subjects had no experience of the use of any illicit drugs, and had no history of mental disorders, including substance-related disorders, according to the DSM-IV. Both groups reported similar occasional smoking and drinking habits, and none of the subjects matched the DSM-IV criteria for either nicotine- or the alcohol-related disorders. The toluene users were recruited from the Hamamatsu University Hospital, and from three associated hospitals (Hattori Mental Hospital, Shimada Municipal Hospital, and Hamamatsu Neurological Hospital).

The duration of toluene use was defined as the time that had intervened between the initial and the last use of toluene. In cases involving intervals of abstinence exceeding 1 month during the duration of toluene use as defined, these intervals were subtracted from the total length of toluene use. The duration of abstinence from toluene use was defined as the time between the day of the last use of toluene and the day of the ^{1}H MRS examination. Cumulative lifetime exposure to toluene was estimated in milliliters. Among the 12 toluene users, five had been treated with neuroleptics, while the remaining seven toluene users had not previously taken neuroleptics prior to the ^{1}H MRS examination. Current and total lifetime neuroleptic doses in the five toluene users were quantified in chlorpromazine-equivalent dosages (American Psychiatric Association, 1997). In order to establish recent abstinence from toluene use, we regularly tested the subjects for urinary hippuric acid, a biomarker of toluene use (Raikhlin-Eisenkraft *et al*, 2001), using high-performance liquid chromatography, which was carried out according to the standard diagnostic methods. In addition, to verify abstinence from other illicit drugs, we used a rapid immunoassay for the qualitative detection of the metabolites of the following eight classes of drugs: amphetamines (including (±)3,4-methylenedioxymethamphetamine and methamphetamine), barbiturates, benzodiazepines, cocaine, methadone, opiates, tetrahydrocannabinol, and tricyclic antidepressants (Triage 8, Biosite Diagnostics, San Diego, USA). These assessments were also performed on the same day as the ^{1}H MRS examination. Psychiatric symptoms in the toluene users were evaluated using the Brief Psychiatric Rating Scale (BPRS) (Overall and Gorham, 1962) on the day of the ^{1}H MRS study. The assessment was conducted by a trained research psychiatrist blind to the ^{1}H MRS data. After providing the subjects with a complete description of the study, written informed consent was obtained from all participants before entry into the study, in compliance with the procedures of the Ethics Committee of the Hamamatsu University School of Medicine.

Image Acquisition

MRS was performed at the Hamamatsu University Hospital, using a 1.5-T whole-body MR scanner (Signa Horizon; General Electric Medical Systems, Milwaukee, WI, USA) equipped with self-shielded gradient coils. A quadrature, MR bird-cage coil (trans/receive) was used throughout the study. The localized MR spectra were recorded using the point-resolved spatially localized spectroscopy (PRESS) sequence from the bilateral basal ganglia. The RF transmitter frequency was centered at the water resonance frequency (63.88 MHz). A 90° flip angle was determined by varying the RF amplifier gain until a maximal signal consistent with a good slice profile was obtained. The B_0 shim on the 27 ml cubic excited volume was optimized using linear shims to a full-width at half-maximum (FWHM) of <6.4 Hz. Voxel size was 8 cm^3 ($2 \times 2 \times 2$ cm^3). To establish the voxel of interest (VOI) on an MR image, scout views in the proton density images were obtained vertically in the *Z*-axis (Figure 1). Proton density images were acquired because gray matter contrasts well with white matter in this type of imaging study (Sekine *et al*, 2002).

After the location of the VOI had been verified by localized MR imaging, the magnetic field in the VOI was optimized by means of a water signal to establish a linewidth of <3 Hz. The acquisition parameters were as follows: repetition time (TR), 1500 ms; echo time (TE), 40 ms; and acquisition time, 3 min 42 s. Peaks of *N*-acetylaspartate (NAA) (2.0 ppm), creatine plus phosphocreatine (Cr + PCr) (3.0 ppm), choline-containing compounds (Cho) (3.2 ppm), and myo-inositol (MI) (3.6 ppm) were obtained. Data processing were performed using a PROBE/SV-Quant tool (General Electric Medical Systems,

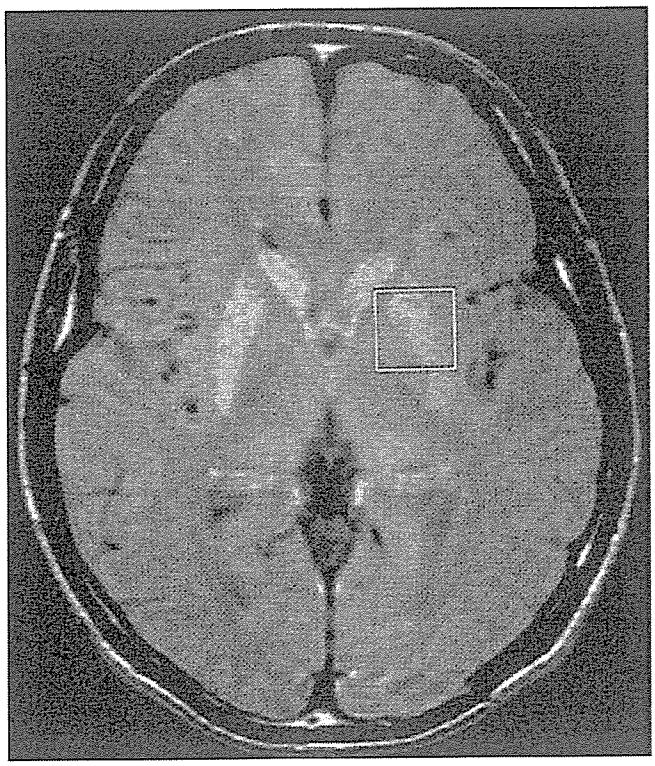

Figure 1 Axial slice proton density MRI showing the typical location of the MRS voxel. The right side of the figure represents the left side of the brain.

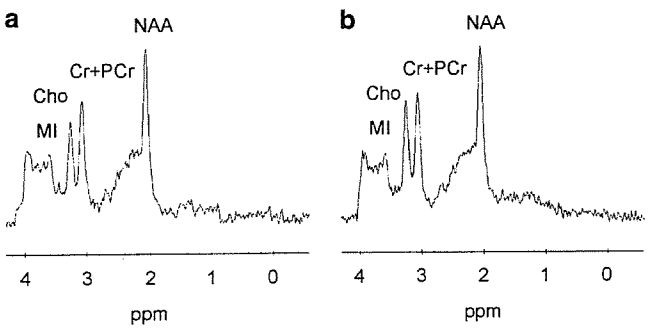

Figure 2 Proton MRS spectra for the right basal ganglia region of (a) a comparison subject and (b) a toluene user. MI, myo-inositol; Cho, choline-containing compounds; Cr + PCr, creatine plus phosphocreatine; NAA, *N*-acetylaspartate.

Milwaukee, WI, USA), which employs a standard nonlinear least-squares algorithm for fitting the observed data. The metabolite ratios were calculated from the fitted peak integrals in the resulting spectra using a method of automatic metabolite peak measurement (Kreis *et al*, 1991; Webb *et al*, 1994). Representative spectra for the right basal ganglia region of a comparison subject and a toluene user are shown in Figure 2. The ratios of NAA/Cr + PCr, MI/Cr + PCr, Cho/Cr + PCr, and Cho/NAA in the toluene users were compared with those of the comparison subjects.

It should be noted that we were unable to completely exclude potential cerebrospinal fluid (CSF) contamination. All measurements were determined by reference to a standard neuroanatomic atlas (Daniels *et al*, 1987), and great care was taken to minimize CSF contamination. However, measurement of tissue water signal from the voxel was too variable owing to a tissue/ventricle artifact to be used to calculate absolute concentrations of metabolites. Accordingly, only the metabolite ratios are reported here.

Statistical Analysis

Student's *t*-test was used for the comparison of the means of the metabolite ratios between toluene users and comparison subjects. The relationships between the metabolite ratios and clinical parameters (ie the duration of toluene use, the duration of abstinence, the lifetime amount of toluene use, the current neuroleptic dose, the lifetime neuroleptic dose, and the BPRS score) were evaluated using Pearson's correlation coefficient. We measured the metabolite ratios in the basal ganglia on both the left and right sides of each subject. The values measured in each of the hemispheres were not naturally independent within the same individual, and separate analyses of the ratios, as measured on each side, would have increased the risk of Type I error due to multiple testing. To avoid such errors, we used repeated measures analysis of variance (ANOVA), in which the repeated measures were the left and right metabolite ratios. In all of the statistical analyses, an alpha level of 0.05 was considered to be significant.

RESULTS

The demographic and clinical characteristics of the toluene users and the comparison subjects are shown in Tables 1

Table 1 Demographic Characteristics of Toluene Users and Comparison Subjects

	Toluene users ($n = 12$)	Comparison subjects ($n = 13$)	Significance
Age (years)	29.6 (6.5)	25.9 (6.3)	NS[a]
Gender (male/female)	9/3	10/3	NS[b]
Duration of use (years)	7.8 (5.1)	—	—
Duration of abstinence (years)	4.9 (4.9)	—	—
Total lifetime exposure of toluene (liters)	2 298 (4 900)	—	—
BPRS total score	16.1 (9.6)	—	—

Data are presented as mean (SD). BPRS, the Brief Psychiatric Rating Scale; NS, nonsignificant.
[a]NS, by *t*-test.
[b]NS, by Fisher's exact test.

Table 2 Clinical Characteristics of Toluene Users

Subject	Age (years)	Sex	Age of first toluene use (years)	Duration of toluene use (years)	Duration of abstinence (years)	Lifetime exposure toluene (ml)	Neuroleptic dose at scanning[a] (mg/day)	Lifetime neuroleptic dose[a] (mg)	BPRS score	Symptoms at time of MRS
1	21	m	15	3	3.5	17 460 000	0	0	5	Auditory hallucinations
2	23	m	15	5	3.0	2 737 500	0	0	14	Persecutory delusions Unusual thought content
3	32	m	23	11	0.3	231 000	0	0	25	Persecutory delusions Emotional apathy
4	36	m	18	12	10.0	912 500	175	1 420 500	24	Emotional apathy
5	32	m	14	6	1.0	3 355 500	400	9000	19	Somatic delusions Emotional apathy
6	18	f	15	1	3.0	14 400	0	0	11	Anxiety Excitement
7	30	f	16	7	7.0	1 404 000	0	0	3	Anxiety
8	41	m	13	17	3.0	602 357	1 827	9 072 000	33	Auditory hallucinations Emotional apathy
9	28	m	15	13	0.1	787 200	100	237 000	27	Somatic delusions Auditory hallucinations Emotional apathy
10	34	f	15	4	14.0	7821	0	0	16	Anxiety Depressive mood
11	32	m	17	3	13.0	16 965	400	677 775	10	Auditory hallucinations Excitement
12	28	m	14	13	1.0	47 400	0	0	6	Emotional apathy

[a]Neuroleptic dosages are in chlorpromazine equivalents.

Table 3 Metabolite Ratios in the Left and Right Basal Ganglia of Toluene Users ($n = 12$) and Comparison Subjects ($n = 13$)

	NAA/Cr+PCr	MI/Cr+PCr	Cho/Cr+PCr[a]	Cho/NAA[b]
Toluene users				
Left basal ganglia	1.41 (0.13)	0.41 (0.08)	0.80 (0.08)	0.57 (0.07)
Right basal ganglia	1.38 (0.10)	0.45 (0.06)	0.82 (0.09)	0.60 (0.09)
Comparison subjects				
Left basal ganglia	1.35 (0.18)	0.47 (0.18)	0.72 (0.07)	0.53 (0.05)
Right basal ganglia	1.44 (0.17)	0.42 (0.08)	0.74 (0.07)	0.52 (0.05)

Data are presented as mean (SD). NAA, *N*-acetylaspartate; Cr+PCr, creatine plus phosphocreatine; MI, myo-inositol; Cho, choline-containing compounds.
[a]$p = 0.006$.
[b]$p = 0.02$ for toluene users *vs* comparison subjects, by repeated measures ANOVA in which the repeated measures were the left and right metabolite ratios.

and 2. No significant difference was observed as regards the distribution of age or sex between the toluene users and the comparison subjects. The mean age of the first inhalation in toluene users was 15.8 years (range: 13–23). While one toluene user had a first-degree relative with alcoholism, none of the other users had any first- or second-degree relatives with any psychiatric disorders. The 12 toluene users, with or without neuroleptic treatment, showed similar clinical symptoms, such as auditory hallucinations, persecutory delusions, and emotional apathy. However, they exhibited no noticeable diminished volition, incongruity of affect, stereotypy, mannerism, or loosening of association, and their interest in social activities and interpersonal relationship were fairly maintained. Among the 12 toluene users, five had been treated with neuroleptics, including chlorpromazine, levomepromazine, haloperidol, risperidone, and quetiapine. The neuroleptics successfully improved psychotic symptoms characterized by delusions or hallucinations, but were less effective for emotional apathy.

The metabolite ratios for the left and right basal ganglia are shown in Table 3. Repeated measures ANOVA revealed no significant interaction of group and laterality (left *vs* right) in the metabolite ratios measured, which suggested that any differences observed between the ratios of the two groups were similar in the left and right basal ganglia. There was no significant difference in the NAA/Cr + PCr ratio between the two groups ($F = 0.001$, $df = 1,23$, $p = 0.98$). When the toluene users were divided into two groups, that is, medicated ($n = 5$) and nonmedicated ($n = 7$), no significant difference between either of these groups and the comparison subjects was found ($F = 0.06$, $df = 1,16$, $p = 0.81$ for the medicated group; $F = 0.06$, $df = 1,18$, $p = 0.81$ for the nonmedicated group). There was also no significant difference in the MI/Cr + PCr ratio between the toluene users and the comparison subjects ($F = 0.09$, $df = 1,23$, $p = 0.77$). The difference between the medicated patients and comparison subjects was not significant, nor was that between the nonmedicated patients and comparison subjects ($F = 0.001$, $df = 1,16$, $p = 0.98$ for the medicated group; $F = 0.57$, $df = 1,18$, $p = 0.11$ for the nonmedicated group). However, the toluene users had significantly higher ratios of Cho/Cr + PCr than did the comparison subjects ($F = 9.10$, $df = 1,23$, $p = 0.006$). A similar significance was also noted in the five medicated ($F = 10.19$, $df = 1,16$, $p = 0.006$) and seven nonmedicated ($F = 4.50$, $df = 1,18$, $p = 0.05$) toluene users as compared with the comparison subjects. The ratio of Cho/NAA was significantly higher in the toluene users compared with that of the comparison subjects ($F = 6.15$, $df = 1,23$, $p = 0.02$). The difference in the ratio between nonmedicated toluene users and comparison subjects was of marginal significance ($F = 4.01$, $df = 1,18$, $p = 0.06$), but the difference between medicated toluene users and the comparison subjects was found to be significant ($F = 6.24$, $df = 1,16$, $p = 0.02$).

There was a significant positive correlation between the Cho/Cr + PCr ratio and the BPRS score on the left side of the basal ganglia ($r = 0.57$, $df = 11$, $p = 0.05$) (Figure 3), whereas such a correlation was not found on the right side ($r = 0.18$, $df = 11$, $p = 0.58$). None of the other clinical variables, that is, the duration of toluene use (left: $r = 0.09$, $df = 11$, $p = 0.79$; right: $r = 0.05$, $df = 11$, $p = 0.87$), the duration of abstinence (left: $r = 0.25$, $df = 11$, $p = 0.44$; right: $r = 0.18$, $df = 11$, $p = 0.57$), the total lifetime exposure to toluene (left: $r = 0.42$, $df = 11$, $p = 0.18$; right: $r = 0.24$, $df = 11$, $p = 0.46$), current neuroleptic dose (left: $r = 0.05$, $df = 11$, $p = 0.87$; right: $r = 0.09$, $df = 11$, $p = 0.78$), or lifetime neuroleptic dose (left: $r = 0.006$, $df = 11$, $p = 0.99$; right: $r = 0.26$, $df = 11$, $p = 0.42$), were correlated with the Cho/Cr + PCr ratio on either side of the basal ganglia. Due to the possibility that the psychiatric symptoms were ameliorated by medication at the time of assessment, we computed the partial correlation coefficient with adjustment for the current neuroleptic dose. As anticipated, a slightly higher correlation emerged between the Cho/Cr + PCr ratio in the left basal ganglia and the BPRS score ($r = 0.65$, $df = 9$, $p = 0.03$), whereas the correlation between Cho/Cr + PCr ratio in the right basal ganglia and the total BPRS score remained nonsignificant ($r = 0.27$, $df = 9$, $p = 0.42$).

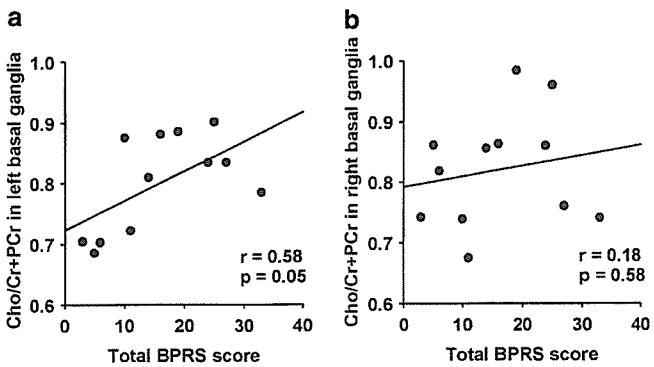

Figure 3 Correlations between clinical variables and values of the Cho/Cr + PCr ratio in the (a) left and (b) right basal ganglia of toluene users ($n = 12$). A significant correlation was found only in the left basal ganglia using Pearson's correlation coefficient.

DISCUSSION

The present study revealed that the ratio of Cho/Cr + PCr in the bilateral basal ganglia of toluene users was significantly higher than the corresponding value in the comparison subjects. Although the possible change in the Cr + PCr level, as reference, might have modified or obscured actual alterations in the primary metabolites, the Cho/NAA ratio, as well as the Cho/Cr + PCr ratio, was significantly higher in the basal ganglia of the toluene users compared with that of the comparison subjects. Therefore, it follows that changes in the Cho/Cr + PCr ratio may arise from an elevation of Cho in the basal ganglia of toluene users. To our knowledge, this is the first examination of the effects of toluene on the MRS measures of brain chemicals. The Cho/Cr + PCr ratio may be a nonspecific marker of toluene-induced biochemical changes in the basal ganglia in long-term toluene users. However, since five of the 12 toluene users examined received neuroleptic medication, the effect of medication on the metabolite ratio should be considered. Indeed, several ^{1}H MRS studies of medicated patients with schizophrenia have shown an increased Cho/Cr + PCr ratio in the caudate nucleus (Ando *et al*, 2002; Bustillo *et al*, 2001), although other studies have not (Heimberg *et al*, 1998; Ohara *et al*, 2000). Consequently, at this point, the effect of neuroleptic medication on the metabolite values of brain Cho/Cr + PCr remains controversial. In this study, a significant increase in the Cho/Cr + PCr ratio was observed, in the seven toluene users who had not been medicated. However, the level of significance demonstrated in the seven nonmedicated users was of borderline significance ($p = 0.05$), whereas the result was highly significant in the five medicated toluene users ($p = 0.006$). Therefore, the use of neuroleptic medication may have exerted some effect on the elevation of the Cho/Cr + PCr ratio in the participants of this study.

The peak of choline-containing compounds on ^{1}H MRS reflects the concentrations of free choline, phosphocholine, and glycerophosphorylcholine (Miller *et al*, 1996; Stanley *et al*, 2000). The compounds responsible for the choline peak are associated with membrane phospholipids, and have been reported to be increased in a variety of human pathologies that are characterized by increased membrane phospholipid turnover such as demyelinating processes and gliosis; examples include multiple sclerosis (Tartaglia *et al*,

2002), HIV-related brain disease (Chang *et al*, 1999), dementia (Pfefferbaum *et al*, 1999), and epilepsy (Lundbom *et al*, 2001). In animal studies, Gerasimov *et al* (2002) have recently demonstrated using PET that rapid uptake and clearance of radioactivity of [^{11}C]toluene into specific regions of the brain take place, especially in the striatum, and this effect is thought to be the high lipid solubility of this agent. In addition, both acute and long-term exposure of rats to toluene have been shown to alter membrane composition and membrane fluidity (Edelfors and Ravn-Jonsen, 1989; Kyrklund *et al*, 1987; Lebel and Schatz, 1990; von Euler *et al*, 1990). Two post-mortem studies of the brains of toluene users have reported diffuse demyelination in the subcortical white matter, in addition to the gliosis of white and/or gray matter (Escobar and Aruffo, 1980; Rosenberg *et al*, 1988). In human MRI studies, T2-weighted images of toluene abusers showed hypointensity in the basal ganglia and thalamus (Aydin *et al*, 2002; Filley *et al*, 1990; Rosenberg *et al*, 1988; Unger *et al*, 1994), and this type of hypointensity has been suggested to be associated with changes in myelin metabolism (Aydin *et al*, 2002; Rosenberg *et al*, 1988). In addition, demyelinating lesions are thought to contribute to the increase in the Cho/Cr ratio in a patient with multiple sclerosis (Arnold *et al*, 1992). Taken together, the elevated Cho/Cr + PCr ratio in the basal ganglia observed in abstinent toluene users in this study may have been reflective of a long-lasting abnormality in membrane phospholipid metabolism, in particular, demyelination.

The elevation of Cho/Cr + PCr ratios in the left, but not in the right, basal ganglia was significantly correlated with the severity of psychiatric symptoms as measured by the BPRS. The reason for this lateralized dysfunction of the brain in toluene users is not known. However, it is generally accepted that left lateralized dysfunction or structural changes can be observed in neuropsychiatric disorders such as schizophrenia (Hietala *et al*, 1995; Petty, 1999; Reynolds, 1983). In this study, an elevation in the Cho/Cr + PCr ratio was noted among those who had stopped using toluene for 4.9 years on average. Therefore, the abnormalities in membrane phospholipid metabolism observed in these toluene users may be persistent and may participate in the pathogenesis of protracted psychiatric symptoms. Although no prior studies have examined the relationship between psychiatric symptoms and neurochemical alterations in toluene users, there is some evidence linking membrane abnormalities with psychiatric symptoms in patients with schizophrenia (Fenton *et al*, 2000; Fukuzako *et al*, 1996; Ross *et al*, 1997).

In this study, no significant difference was found in NAA/Cr + PCr ratios between the toluene users and the comparison subjects. This finding was not altered when the administration of neuroleptic medication was taken into account. In addition, since NAA has been widely used as a marker of neuronal density (Miller, 1991; Simmons *et al*, 1991; Tsai and Coyle, 1995), our results suggest that toluene abusers may be spared from neuronal loss in the basal ganglia. Indeed, this view is in line with the finding that there was no difference in the MI/Cr + PCr ratio between toluene users and comparison subjects in this study. Since MI is considered to be a marker of glial response (Brand *et al*, 1993), a finding of no change in the MI/Cr + PCr ratio may represent the absence of neuronal damage in toluene users. Histological studies of rats chronically exposed to toluene have shown no significant neuronal loss in the neocortex or cerebellum (Korbo *et al*, 1993; Ladefoged *et al*, 1991), although one study has shown a reduction in the density of neurons in the hippocampus of toluene-exposed rats (Korbo *et al*, 1996). Furthermore, an enzyme immunoassay study using γ-enolase and calbindin-D28k as neural cell markers showed no quantitative changes in the cerebrum of rats after exposure to toluene (Huang *et al*, 1992). In post-mortem case reports about two toluene users who abused toluene for 12 and 20 years, respectively, one patient was reported to have neuronal loss in the cerebrum, basal ganglia, and cerebellum (Escobar and Aruffo, 1980), while in the other case, no neuronal loss was detected in the cerebrum or cerebellum (Rosenberg *et al*, 1988). Generally, neural cells appear less likely to be compromised by exposure to toluene, although very high doses of toluene can damage neural cells (Hansson *et al*, 1988). However, vulnerability to toluene exposure may vary in different regions of the brain. Therefore, the result showing no change in the NAA/Cr + PCr ratio in our study does not exclude the possibility of neuronal damage occurring in brain regions other than the basal ganglia.

A worldwide comprehensive survey has shown that the majority of toluene users start inhaling toluene when they are teenagers (Kozel *et al*, 1995; Neumark *et al*, 1998). In accordance with that survey, all but one of our toluene users (with the exception starting toluene inhalation at the age of 23 years) began to take toluene while still a teenager, that is, under 18 years of age. Furthermore, the mean age of initiation of toluene use in this study (about 16 years) was far earlier than the mean age of onset of schizophrenia, which has been shown to be in the early 20s (Bromet *et al*, 1995). Although we cannot rule out the possibility that the use of toluene precipitates schizophrenia in vulnerable individuals, as pointed earlier, none of the toluene users had a family history of major psychosis. However, the toluene users in the present study had psychotic symptoms akin to those related to the paranoid type of schizophrenia, namely, auditory hallucinations and persecutory delusions. Nonetheless, it may be of note that none of our toluene users showed avolition, alogia, inappropriate affect, stereotypy, mannerism, or social withdrawal, which are frequently seen in patients with schizophrenia. In general, these findings suggest that the toluene-related psychiatric condition may differ from that of schizophrenia.

In summary, we demonstrated an elevation of the Cho/Cr + PCr ratio in the basal ganglia of recreational toluene users, and this finding provides evidence of an abnormality in membrane metabolism. In addition, this membrane disturbance was associated with the emergence and persistence of psychiatric symptoms in toluene users. However, our results should be considered as preliminary due to the small sample size of the present study.

ACKNOWLEDGEMENTS

This work was supported by a Research Grant (16A) for Nervous and Mental Disorders from the Ministry of Health Labor and Welfare, a grant from Japan Society for the

Promotion of Science, a Grant-in-Aid for the Center of Excellence (COE) from the Ministry of Education, Culture, Sports, Science and Technology, Japan, and the Stanley Foundation.

REFERENCES

American Psychiatric Association (1997). Practice guideline for the treatment of patients with schizophrenia. *Am J Psychiatry* **154**: 1–63.

Ando K, Takei N, Matsumoto H, Iyo M, Isoda H, Mori N (2002). Neural damage in the lenticular nucleus linked with tardive dyskinesia in schizophrenia: a preliminary study using proton magnetic resonance spectroscopy. *Schizophr Res* **57**: 273–279.

Arnold DL, Matthews PM, Francis GS, O'Connor J, Antel JP (1992). Proton magnetic resonance spectroscopic imaging for metabolic characterization of demyelinating plaques. *Ann Neurol* **31**: 235–241.

Aydin K, Sencer S, Demir T, Ogel K, Tunaci A, Minareci O (2002). Cranial MR findings in chronic toluene abuse by inhalation. *AJNR Am J Neuroradiol* **23**: 1173–1179.

Brand A, Richter-Landsberg C, Leibfritz D (1993). Multinuclear NMR studies on the energy metabolism of glial and neuronal cells. *Dev Neurosci* **15**: 289–298.

Bromet EJ, Dew MA, Eaton W (1995). Epidemiology of psychosis with special reference to schizophrenia. In: Tsuang MT, Tohen M, Zahner GEP (eds). *Textbook in Psychiatric Epidemiology*. John Wiley & Sons: New York. pp 283–300.

Bustillo JR, Lauriello J, Rowland LM, Jung RE, Petropoulos H, Hart BL *et al* (2001). Effects of chronic haloperidol and clozapine treatments on frontal and caudate neurochemistry in schizophrenia. *Psychiatry Res* **107**: 135–149.

Chang L, Ernst T, Leonido-Yee M, Walot I, Singer E (1999). Cerebral metabolite abnormalities correlate with clinical severity of HIV-1 cognitive motor complex. *Neurology* **52**: 100–108.

Cintra A, Aguirre JA, Andbjer B, Finnman UB, Hagman M, Agnati LF *et al* (1999). Subchronic toluene exposure in low concentrations produces signs of reduced dysfunction in the 6-hydroxydopamine lesioned nigrostriatal dopaminergic system of the rat. *Neurosci Lett* **274**: 5–8.

Daniels DL, Haughton VM, Naidich TP (1987). *Cranial and Spinal MRI: An Atlas and Guide*. Raven Press: New York.

Edelfors S, Ravn-Jonsen A (1989). The effect of toluene exposure for up to 18 months (78 weeks) on the (Ca^{2+}/Mg^{2+})ATPase and fluidity of synaptosomal membranes isolated from rat brain. *Pharmacol Toxicol* **65**: 140–142.

Escobar A, Aruffo C (1980). Chronic thinner intoxication: clinicopathologic report of a human case. *J Neurol Neurosurg Psychiatry* **43**: 986–994.

Fenton WS, Hibbeln J, Knable M (2000). Essential fatty acids, lipid membrane abnormalities, and the diagnosis and treatment of schizophrenia. *Biol Psychiatry* **47**: 8–21.

Filley CM, Heaton RK, Rosenberg NL (1990). White matter dementia in chronic toluene abuse. *Neurology* **40**: 532–534.

First MB, Spitzer RL, Gibbon M, Williams JB (1996). *Structured Clinical Interview for DSM-IV Axis I Disorders (SCID), Non Patient Version*. Biometrics Research. New York State Psychiatric Institute: New York.

Flanagan RJ, Ives RJ (1994). Volatile substance abuse. *Bull Narcotics* **46**: 49–78.

Fukuzako H, Fukuzako T, Takeuchi K, Ohbo Y, Ueyama K, Takigawa M *et al* (1996). Phosphorus magnetic resonance spectroscopy in schizophrenia: correlation between membrane phospholipid metabolism in the temporal lobe and positive symptoms. *Prog Neuropsychopharmacol Biol Psychiatry* **20**: 629–640.

Gerasimov MR, Ferrieri RA, Schiffer WK, Logan J, Gatley SJ, Gifford AN *et al* (2002). Study of brain uptake and biodistribution of [^{11}C]toluene in non-human primates and mice. *Life Sci* **23**: 2811–2828.

Hansson E, von Euler G, Fuxe K, Hansson T (1988). Toluene induces changes in the morphology of astroglia and neurons in striatal primary cell cultures. *Toxicology* **49**: 155–163.

Heimberg C, Komoroski RA, Lawson WB, Cardwell D, Karson CN (1998). Regional proton magnetic resonance spectroscopy in schizophrenia and exploration of drug effect. *Psychiatry Res* **83**: 105–115.

Hietala J, Syvalahti E, Vuorio K, Rakkolainen V, Bergman J, Haaparanta M *et al* (1995). Presynaptic dopamine function in striatum of neuroleptic-naive schizophrenic patients. *Lancet* **346**: 1130–1131.

Hillefors-Berglund M, Liu Y, von Euler G (1995). Persistent, specific and dose-dependent effects of toluene exposure on dopamine D_2 agonist binding in the rat caudate-putamen. *Toxicology* **100**: 185–194.

Hormes JT, Filley CM, Rosenberg NL (1986). Neurologic sequelae of chronic solvent vapor abuse. *Neurology* **36**: 698–702.

Huang J, Asaeda N, Takeuchi Y, Shibata E, Hisanaga N, Ono Y *et al* (1992). Dose[-]dependent effects of chronic exposure to toluene on neuronal and glial cell marker proteins in the central nervous system of rats. *Br J Ind Med* **49**: 282–286.

Ives RJ (2000). Disorders relating to the use of volatile substances. In: Gelder MG, Lopez-Ibor JJ, Andreasen NC (eds). *New Oxford Textbook of Psychiatry*. Oxford University Press: New York. pp 546–550.

Korbo L, Andersen BB, Ladefoged O, Moller A (1993). Total numbers of various cell types in rat cerebellar cortex estimated using an unbiased stereological method. *Brain Res* **609**: 262–268.

Korbo L, Ladefoged O, Lam HR, Ostergaard G, West MJ, Arlien-Soborg P (1996). Neuronal loss in hippocampus in rats exposed to toluene. *Neurotoxicology* **17**: 359–366.

Kozel N, Sloboda Z, Rosa M (1995). Epidemiology of inhalant abuse. An international perspective. *NIDA Res Monograph* **148**, NIH, Public #95–3831. Department of Health and Human services: Rockville, MD (published online, at http://www.drugabuse.gov/pdf/monographs/148.pdf).

Kreis R, Farrow N, Ross BD (1991). Localized ^{1}H NMR spectroscopy in patients with chronic hepatic encephalopathy. Analysis of changes in cerebral glutamine, choline and inositols. *NMR Biomed* **4**: 109–116.

Kyrklund T, Kjellstrand P, Haglid K (1987). Brain lipid changes in rats exposed to xylene and toluene. *Toxicology* **45**: 123–133.

Ladefoged O, Strange P, Moller A, Lam HR, Ostergaard G, Larsen JJ *et al* (1991). Irreversible effects in rats of toluene (inhalation) exposure for six months. *Pharmacol Toxicol* **68**: 384–390.

Lebel CP, Schatz RA (1990). Altered synaptosomal phospholipid metabolism after toluene: possible relationship with membrane fluidity, Na^+,K^+-adenosine triphosphatase and phospholipid methylation. *J Pharmacol Exp Ther* **253**: 1189–1197.

Lundbom N, Gaily E, Vuori K, Paetau R, Liukkonen E, Rajapakse JC *et al* (2001). Proton spectroscopic imaging shows abnormalities in glial and neuronal cell pools in frontal lobe epilepsy. *Epilepsia* **42**: 1507–1514.

Miller BL (1991). A review of chemical issues in ^{1}H NMR spectroscopy: *N*-acetyl-L-aspartate, creatine and choline. *NMR Biomed* **4**: 47–52.

Miller BL, Chung L, Booth R, Ernst J, Cornford M, Nikas D *et al* (1996). *In vivo* ^{1}H MRS choline correlation with *in vitro* chemistry/histology. *Life Sci* **58**: 1929–1935.

Morton HG (1987). Occurrence and treatment of solvent abuse in children and adolescents. *Pharmacol Ther* **33**: 449–469.

Neumark YD, Delva J, Anthony JC (1998). The epidemiology of adolescent inhalant drug involvement. *Arch Pediatr Adolesc Med* **152**: 781–786.

Ohara K, Isoda H, Suzuki Y, Takehara Y, Ochiai M, Takeda H (2000). Proton magnetic resonance spectroscopy of lenticular nuclei in simple schizophrenia. *Prog Neuropsychopharmacol Biol Psychiatry* **24**: 507–519.

Overall JE, Gorham DR (1962). The Brief Psychiatric Rating Scale. *Psychol Rep* **10**: 799–812.

Petty RG (1999). Structural asymmetries of the human brain and their disturbance in schizophrenia. *Schizophr Bull* **25**: 121–139.

Pfefferbaum A, Adalsteinsson E, Spielman D, Sullivan EV, Lim KO (1999). *In vivo* brain concentrations of *N*-acetyl compounds, creatine, and choline in Alzheimer disease. *Arch Gen Psychiatry* **56**: 185–192.

Raikhlin-Eisenkraft B, Hoffer E, Baum Y, Bentur Y (2001). Determination of urinary hippuric acid in toluene abuse. *J Toxicol Clin Toxicol* **39**: 73–76.

Reynolds GP (1983). Increased concentrations and lateral asymmetry of amygdala dopamine in schizophrenia. *Nature* **305**: 527–529.

Rosenberg NL, Grigsby J, Dreisbach J, Busenbark D, Grigsby P (2002). Neuropsychologic impairment and MRI abnormalities associated with chronic solvent abuse. *J Toxicol Clin Toxicol* **40**: 21–34.

Rosenberg NL, Kleinschmidt-DeMasters BK, Davis KA, Dreisbach JN, Hormes JT, Filley CM (1988). Toluene abuse causes diffuse central nervous system white matter changes. *Ann Neurol* **23**: 611–614.

Ross BM, Hudson C, Erlich J, Warsh JJ, Kish SJ (1997). Increased phospholipid breakdown in schizophrenia. Evidence for the involvement of a calcium-independent phospholipase A2. *Arch Gen Psychiatry* **54**: 487–494.

Sekine Y, Minabe Y, Kawai M, Suzuki K, Iyo M, Isoda H *et al* (2002). Metabolite alterations in basal ganglia associated with methamphetamine-related psychiatric symptoms: a proton MRS study. *Neuropsychopharmacology* **27**: 453–461.

Simmons ML, Frondoza CG, Coyle JT (1991). Immunocytochemical localization of *N*-acetyl-aspartate with monoclonal antibodies. *Neuroscience* **45**: 37–45.

Stanley JA, Pettegrew JW, Keshavan MS (2000). Magnetic resonance spectroscopy in schizophrenia: methodological issues and findings—Part I. *Biol Psychiatry* **48**: 357–368.

Tartaglia MC, Narayanan S, De Stefano N, Arnaoutelis R, Antel SB, Francis SJ *et al* (2002). Choline is increased in pre-lesional normal appearing white matter in multiple sclerosis. *J Neurol* **249**: 1382–1390.

Tsai G, Coyle JT (1995). *N*-acetylaspartate in neuropsychiatric disorders. *Prog Neurobiol* **46**: 531–540.

Unger E, Alexander A, Fritz T, Rosenberg N, Dreisbach J (1994). Toluene abuse: physical basis for hypointensity of the basal ganglia on T2-weighted MR images. *Radiology* **193**: 473–476.

Webb PG, Sailasuta N, Kohler SJ, Raidy T, Moats RA, Hurd RE (1994). Automated single-voxel proton MRS: technical development and multisite verification. *Magn Reson Med* **31**: 365–373.

von Euler G, Fuxe K, Bondy SC (1990). Ganglioside GM1 prevents and reverses toluene-induced increases in membrane fluidity and calcium levels in rat brain synaptosomes. *Brain Res* **508**: 210–214.

von Euler G, Ogren SO, Li XM, Fuxe K, Gustafsson JA (1993). Persistent effects of subchronic toluene exposure on spatial learning and memory, dopamine-mediated locomotor activity and dopamine D_2 agonist binding in the rat. *Toxicology* **77**: 223–232.

von Euler M, Pham TM, Hillefors M, Bjelke B, Henriksson B, von Euler G (2000). Inhalation of low concentrations of toluene induces persistent effects on a learning retention task, beam-walk performance, and cerebrocortical size in the rat. *Exp Neurol* **163**: 1–8.